Summer 2022

Using coherence and interference to study the few body dynamics in simple atomic collisions systems

Sujan Bastola

Department: Physics

USING COHERENCE AND INTERFERENCE TO STUDY THE FEW BODY DYNAMICS IN SIMPLE ATOMIC COLLISIONS SYSTEMS

by

SUJAN BASTOLA

A DISSERTATION

Presented to the Graduate Faculty of the

MISSOURI UNIVERSITY OF SCIENCE AND TECHNOLOGY

In Partial Fulfillment of the Requirements for the Degree

DOCTOR OF PHILOSOPHY

in

PHYSICS

2022

Approved by:

Michael Schulz, Advisor
Marco Cavaglia
Daniel Fischer
Anh-Thu Le
Sanjay Madria

PUBLICATION DISSERTATION OPTION

This dissertation consists of the following two articles, formatted in the style used by the Missouri University of Science and Technology:

Paper I, found on pages 11–33, has been published in *Physical Review A*.

Paper II, found on pages 34–52, has been submitted to *the Journal of Physics B*.

ABSTRACT

Atomic Collision experiments are best suited to sensitively test the few-body dynamics of simple systems. The few-body dynamics, in turn, can be sensitively affected by interference effects. However, an important requirement to observe interference effects in atomic scattering experiments is that the incoming projectile beam must be coherent. The coherence properties of the incoming projectile can be controlled by the geometry of the collimating slit placed before the target. We performed a kinematically complete experiment where a 75 keV proton beam is crossed with a molecular hydrogen beam to study the dissociative capture process. The motivation for this project was to explain a π-phase shift found in the interference pattern observed in a previous experiment. To this end the recoil-ion momentum resolution was improved by a factor of 5 and the statistics by an order of magnitude. As a result, we got a pronounced interference pattern in the FDCS as compared to previous data. The differential cross-section in KER showed that the phase shift is not constant at π, but rather changes with θ_p. It is π for relatively small θ_p, almost 0 for large θ_p, and is independent of the KER. In another project we studied p + He collisions to extract the incoherent cross section very close to the velocity matching regime. While in a previous experiment with a coherent beam a double peak structure was observed, we expected a single peak structure in the FDCS in the current experiment. The double peak structure in the coherent case (past experiment) was explained as an interference structure between first and higher order interactions (one of which is PCI). This interpretation is indeed supported by our observation of only a single peak in the incoherent case. It is further supported, at least qualitatively, by a theoretical calculation.

ACKNOWLEDGEMENTS

First, I would like to thank from the bottom of my heart my advisor, Dr. Michael Schulz, for giving me an opportunity to excel in his AMO Physics lab. His continuous support, encouragement, and guidance are the key to my success. His expertise and broad knowledge in the field have not only helped me master AMO Physics but also inspired me to be a good physicist. Secondly, I would like to express my gratitude to my dissertation committee member, Dr. Fischer, who allowed me to volunteer in his Laser lab and learn cutting-edge research techniques. I would also like to thank rest of my Ph.D. dissertation committee members, Dr. Marco Cavaglia, Dr. Anh Thu Le, and Dr. Sanjay Madria, for their valuable suggestions and recommendations. It would be unfair if I miss thanking Dr. Ahmad Hasan. I learned a lot of coding and technical stuff from him which would be useful throughout my life.

I would also like to thank my friends and mentors, Dr. Chandramani Adhikari, Kapil Sharma, Dr. Madhav Dhital, Dr. Ramaz Lomsadze, Dr. Manoj K. Jha, Aaron, Trevor Voss, Jacob Davis, Shruti Majumdar, Kevin Romans and Kyle Foster, for their continuous support and guidance. Also, I appreciate continuous help from Dr. Thomas Vojta, Pam, Jan, Andy Stuffs, and Ron Woody. I would not be able to achieve this without immense support and care from my family. Last but not the least, I would like to thank again a very important member of my family, my wife, Archana Dhungana, for her continuous support, care, and lots of things that I cannot express in words. I will forever be in debt to my family and my advisor for all this.

TABLE OF CONTENTS

LIST OF ILLUSTRATIONS

SECTION Page

1. INTRODUCTION

At the root of all research activities in Physics is the goal to understand nature. To this end, two fundamental questions need to be addressed. We need to obtain a complete understanding of the fundamental forces acting in nature which are: gravitational, weak, electromagnetic, and strong forces. All these fundamental forces are mediated by the exchange of virtual particles called gauge bosons. This mediation of forces among particles is a two-body process because these gauge bosons can only be emitted by one particle and absorbed by one particle at a time. Of these four forces, the electromagnetic force is the only one that is essentially completely understood. Another question is how systems containing more than two particles develop under the influence of these pairwise acting forces? The problem is that the Schrödinger equation (Dirac equation in relativistic cases) is not analytically solvable for more than two particles interacting with each other. This gives rise to one of the most fundamentally important and yet unsolved problems in physics, famously known as the Few-Body Problem (FBP). To solve this problem, theory must resort to heavy modeling efforts and dynamic systems, like fragmentation processes, are particularly challenging to model. These theoretical models must be tested by detailed experimental data. For stationary systems which are characterized by those states of a quantum system that do not change with the evolution of time, accurate solutions can be obtained by using numerical models like the Hartree-Fock model [1]. However, for dynamic few-body systems that evolve with time, solving the FBP is much more challenging.

Atomic collision experiments are particularly well suited for testing the few body dynamics due to two reasons [21-23]. First, the underlying force in atomic systems, the electromagnetic interaction, is essentially understood. Therefore, experiments on atomic systems directly test the description of the few-body dynamics as the description of the force is under control. In contrast, the forces acting in a nuclear system are not nearly as well understood. Therefore, it is not clear whether experiments investigating nuclear systems test the theoretical description of the nuclear force or of the few-body dynamics. Second, in atomic systems relatively small particle numbers (3-5) can be investigated. Therefore, kinematically complete experiments, which offer the most sensitive tests of theory are feasible. These experiments allow us to extract fully differential cross sections (FDCS). In contrast, solid-state systems usually involve particle numbers of the order of Avogadro's number, for which kinematically complete experiments are obviously not possible. Here, only statistically averaged or collective quantities can be measured which does not provide a sensitive test of theory. Among the large variety of reactions that can occur in atomic collision processes e.g., ionization, excitation, capture, etc., ionization is most befitted to study the few body problem because the final state involves three unbound particles namely the recoil ion, the scattered projectile, and the ejected electron. In the case of capture and excitation, there are only two independently moving particles in the final state. Although in electron impact ionization there is very good agreement between experiment and theory in the case of one or two-electron targets, ion impact collisions experiments are still not well understood [9-11, 20]. Ion impact experiments are much more challenging because the larger projectile mass as compared to electrons leads to tiny scattering angles and energy losses compared with the initial projectile energy. From a

theoretical point of view, one major challenge is that due to the large mass of ions a very large number of angular momentum states contribute to the scattered projectile state [36]. The experimental challenges were solved by developing cold target recoil-ion momentum spectroscopy (COLTRIMS) where we can directly measure the momenta of recoil ions and ejected electrons or scattered projectiles for light ions at small and intermediate speeds to perform kinematically complete experiments [24-27].

A large variety of theoretical models have been used over the years to describe the few-body dynamics in charged particle interactions. These all can be categorized into two broad groups namely perturbative and non-perturbative models. In atomic collision experiments, the perturbation parameter (η), which is the charge to speed ratio of the projectile, is an important parameter. For collisions with small η measured cross-sections are often well reproduced by both perturbative and non-perturbative approaches. Especially for electrons ejected into the scattering plane which is spanned by the initial momentum vector p_0 and the momentum transfer vector q agreement tends to be better than for other geometries. For this specific regime, experimental results are even reproduced quite well by the rather simple First-Born Approximation (FBA) model [9-11]. Previously it was believed that in this kinematic regime collision dynamics are well understood even in the case of electron emission outside the scattering plane. But later, FDCS measurements suggested that there are significant discrepancies in the case of ion-impact collisions outside the scattering plane even for η as small as 0.1 [15-20].

Surprisingly, semi-classical calculations like the convolution of the FBA with classical elastic scattering [22] reproduced the experimental data much better. It was, therefore, suggested that the discrepancies may be related to an unrealistic description of

the projectile coherence properties. In all QM calculations, they considered a completely delocalized projectile beam, which means the projectile beam is treated fully coherent while semi-classical calculations assume classical localized trajectories. Usually, the projectile coherence properties are somewhere between these two extremes and the incoming projectile should be described by a wave packet of finite width. The beam is coherent when the width of the projectile wave packet is large compared to the dimension of the diffracting object. But in practice, ionic projectiles are massive and relatively fast, so compared to electrons they tend to be better localized because of their tiny de Broglie wavelength. Therefore, for fast heavy-ion impact, the wave packet tends to have a much narrower width than for electrons.

One important consequence of a small coherence length is that interference patterns, which may be predicted by theory, are not observable experimentally. To test the role of coherence experimentally with good precision it is, therefore, advantageous to study a process for which it is known that an interference structure is present for a coherent beam. One such process is projectile scattering off a diatomic molecular target [33-35]. There, coherence effects were indeed identified by measuring scattering cross-sections for projectiles with a small and a large coherence length [31]. In analogy to classical optics, the transverse coherence length is determined by the geometry of a collimating slit placed before the target by:

$$\Delta x = \lambda \left[\frac{L}{2a} \right] \tag{1}$$

Here, a is the width of the collimating slit, L is the distance of the slit from the target and λ is the de-Broglie wavelength of the projectile. The experiment by Egodapitiya et al. [31]

was performed for 2 slit distances and interference was observed for the large, but not for the small slit distance.

This dissertation used coherence and interference effects to investigate 2 questions that arose from past studies. First, in the scattering of ions from di-atomic molecules, two-center interference effects are routinely observed and often well reproduced by theory. However, in some cases, a π phase shift was observed [14, 30]. This was convincingly explained by parity conservation. The most detailed study of two-center interference effects was performed in a kinematically complete experiment on 10 keV H_2^+ + He

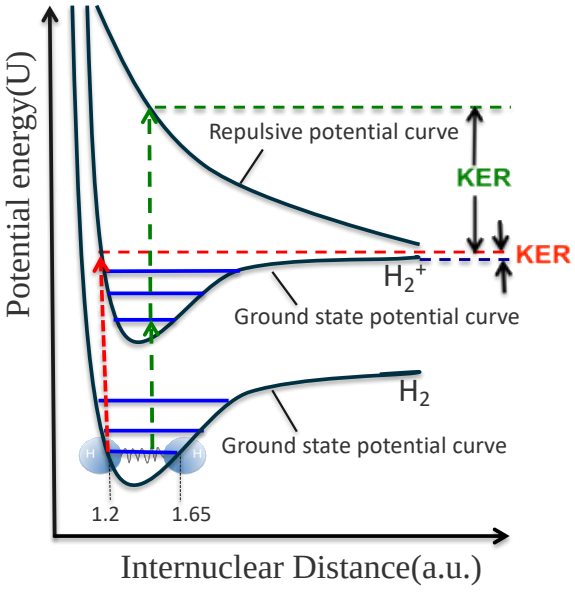

Figure 1.1. Potential Energy diagram of a Hydrogen molecule. Green-colored transitions represent the electronic vibrational channel, and the red-colored transition is for the vibrational dissociation channel

collisions [30]. The FDCS were presented as a function of recoil-ion momentum for fixed Kinetic energy and molecular orientation. They got a very pronounced interference pattern

which was phase-shifted by π as compared to the theoretical two-center interference term [13]. This phase shift was convincingly explained by parity conservation as they selected electron transfer from the target to the dissociative $2p\sigma_u$ state of the projectile indicated by the upper green- colored transition in Figure 1.1. Several studies were then performed to study this π phase shift [8,14,45], some confirmed the phase shift, but others did not. This conflict has not been resolved yet. Details are given in Paper I in the publication section.

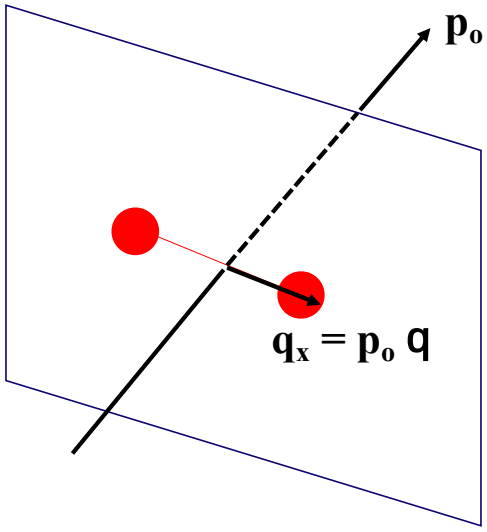

Figure 1.2. Parallel molecular orientation (q is parallel to D).

In dissociative capture, there is another channel in addition to the electronic dissociation channel which is known as a ground state [46] or vibrational dissociation [34] indicated by the red-colored transition in Figure 1.1. Unlike the electronic transition, vibrational dissociation is caused by the excitation of the nuclear motion to a vibrational continuum state which means the molecular ion (H2+ in case of H2 target) remains in the ground state if we disregard the vibrational motion [35]. Although there is no switch in

symmetry of the molecular state in the vibrational dissociation channel, a π phase shift was observed in FDCS for vibrational dissociation following target ionization in 200 eV e^- + H_2 [46] as well as for vibrational dissociation following electron capture in 75 keV p + H_2 collisions [34]. There, the explanation for the π-phase shift based on parity conservation does not hold. Another study by Lamichhane et al. didn't provide an explanation for the observed π phase in the case of the parallel molecular orientation illustrated in Figure 1.2., and in addition, there were significant quantitative disagreements between experiment and theory at large scattering angles. Also, neither they had sufficient statistics nor sufficient resolution to analyze the data differential in KER. The motivation behind my first project (described in Paper I) was to investigate the process with improved resolution and statistics. In this project, we did a fully differential investigation of two-center interference in dissociative capture in p + H_2 collision. The experimental arrangement is similar to Lamichhane et al. [34] except we changed the extraction voltage of the recoil ions from 500 V to 100V which improved our resolution by a factor of 5. Furthermore, we collected 10 times as much true coincident data as compared in the previous project. The interference structure in FDCS we extracted was more pronounced as compared to Lamichhane et al. FDCS data which are described in detail in the publication section (Paper I).

The second project is related to the question that arose from past studies related to fully differential angular distributions of electrons ejected in ionization by ion impact near the matching velocity (i.e., the electron speed is close to the projectile speed). There, a previously unobserved structure in the forward direction was found which was attributed to a higher-order process known as PCI. This process involves at least two interactions

between the projectile and the target electron. In the first step, the projectile transfers sufficient energy to the target electron so that it is excited to the continuum. In the outgoing part of the collision, the scattered projectile and ejected electron then attract each other focusing both to the initial projectile direction. For this to be possibly in order to conserve momentum, either the electron or the projectile has to be redirected by an interaction with the target nucleus before the second projectile interaction can occur [58]. This focusing effect maximizes when the velocity of the ejected electron becomes very close to the projectile velocity, and this is called the velocity matching region. The most detailed information about the reaction dynamics in atomic collisions can be extracted from fully differential cross sections (FDCS) measured in kinematically complete experiments. The FDCS study reported in [58] found a double peak structure in the velocity matching regime in the electron ejection angular dependence. One peak, the binary peak, is nearly in the direction of the momentum transfer (indicated by an upward arrow in Figure 1.3) and the second peak, the forward peak, is in the initial projectile direction. However, due to PCI, the binary peak is shifted towards the forward direction as we can see in Figure 1.3 [58].

In a classical picture, the double-peak structure shown in Figure 1.3 is not straightforward to explain as the separate forward peak and forward-shifted binary peak are the results of the same mechanism, PCI. In other words, the existence of the forward peak and the forward shifted binary peak is due to the attraction of the ejected electrons by the projectile in the direction of the beam axis. This attraction results in the shift of both structures with respect to the direction of momentum transfer (q). If θq represents the direction of momentum transfer **q** then we can say that the forward peak is shifted by 100 % with respect to θ_q while the shift in binary peak is only about 20% of θ_q.

The question then arises, why a shift of 100% and 20% is likely and a shift of 50% (where we have a minimum) is unlikely? Classically, it is not clear that this question can be answered. On the other hand, in quantum mechanics, a possible explanation is that this minimum is the result of destructive interference between different transition amplitudes

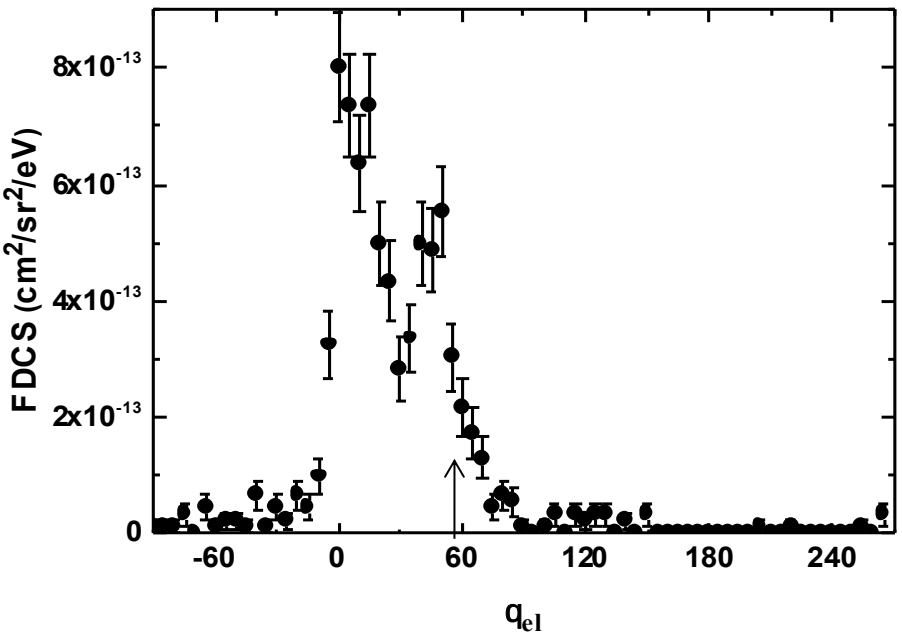

Figure 1.3. Fully differential cross sections for electron ejected into the scattering plane as a function of scattering angle for 60 eV energy loss for $p+H_2$ collision.

leading to the same final state [58]. One important requirement for interference to be observable is that the incoming projectile wave must be coherent. As discussed earlier this means that the coherence length must be larger than the dimension of the Helium atom for interference to occur. In this project, we report an FDCS measurement in the velocity matching region where $\Delta x < 1$ a.u. but otherwise identical conditions as in [58]. So, in the current experiment, the proton beam is less coherent as compared to the previous

experiment and we expected a diminishing interference structure. The experimental results and theoretical calculations are described in detail in the publication section of the dissertation (Paper II).

PAPER

I. FULLY DIFFERENTIAL INVESTIGATION OF TWO-CENTER INTERFERENCE IN DISSOCIATIVE CAPTURE IN P+H_2 COLLISIONS

S. Bastola,[1] M. Dhital,[1,*] B. Lamichhane,[1,†] A. Silvus ,[1,‡] R. Lomsadze ,[2] J. Davis,[1] A. Hasan,[3] A. Igarashi,[4] and M. Schulz [1,§]

[1]Physics Dept. and LAMOR, Missouri University of Science & Technology, Rolla, Missouri 65409, USA

[2]Dept. of Exact and Natural Science, Tbilisi State University, Tbilisi 0179, Georgia

[3]Dept. of Physics, UAE University, P.O. Box 15551, Al Ain, Abu Dhabi, UAE

[4]Faculty of Engineering, University of Miyazaki, Miyazaki 889-2192, Japan

[*]Present address: Physics Dept., University of California-Riverside, Riverside, CA 92521. [†]Present address: Earlham College, Richmond, IN 47374.
[‡]Present address: Department of Radiation Oncology, Washington University, St. Louis, MO 63110.
[§]schulz@mst.edu

ABSTRACT

We have measured and calculated fully differential cross sections for vibrational dissociation following capture in 75-keV p + H2 collisions. For a molecular orientation perpendicular to the projectile beam axis and parallel to the transverse momentum transfer we observe a pronounced interference structure. The positions of the interference extrema suggest that the interference term is afflicted with a phase shift which depends on the projectile scattering angle. However, no significant dependence on the kinetic-energy

release was observed. Considerable discrepancies between our calculations and experimental data were found.

1. INTRODUCTION

Already more than six decades ago Tuan and Gerjuoy predicted two-center interference effects in electron capture in $p + H_2$ collisions [1]. Since as a matter of principle it is not possible to distinguish from which atomic center of the molecule the projectile is diffracted, the transition amplitudes for both possibilities have to be added coherently. This can lead to interference structures in the cross sections as a function of parameters which determine the phase angle in the interference term. It took another three decades before such interference structures were experimentally identified in cross sections differential in the molecular alignment for dissociative capture in $O^{8+} + D_2$ collisions [2]. Later, they were also found in double-differential spectra of electrons ejected from H2 by highly charged ion impact [3]. These studies sparked major activities on experiments studying such interference effects in more detail (e.g., Refs. [4–10]).

Perhaps the most detailed study of such interference effects was performed in a kinematically complete experiment on 10-keV H_2^+ + He collisions [5]. There, electron transfer from the target to the dissociative $2p\sigma_u$ state of the projectile was selected. For fixed molecular orientation and kinetic-energy release (KER) the fully differential cross sections (FDCS) were presented as a function of the recoil-ion momentum. Very pronounced interference structures were observed. However, the patterns were afflicted with a phase shift of π relative to the expected theoretical two-center interference term I_2

[11]. This was convincingly explained by parity conservation: the switch of symmetry of the molecular state from gerade to ungerade during the transition must be compensated by a corresponding switch in symmetry of the He atom in its motion relative to the molecular projectile.

The same π-phase shift was also observed in FDCS for target ionization accompanied by projectile excitation to the 2pσu state in 1-MeV H_2^+ + He collisions, which involves the same symmetry switch of the molecular state [9]. On the other hand, no phase shift was found in the cross sections for electron capture accompanied by electronic excitation to a dissociative state of the residual molecular ion in 1.3- MeV p + H_2 collisions [6]. Although this experiment was not strictly state selective, the selected KER range of 5 to 8 eV should have strongly favored dissociation through the 2pπu state. Based on the reasoning of Ref. [5] a π-phase shift was to be expected in the data of Ref. [6] as well. To the best of our knowledge this apparent conflict has not been resolved yet. We do point out, however, that our data for the same process as studied in Ref. [6], but for a projectile energy of 75 keV and a KER range of 5 to 12 eV [12], are consistent with the explanation offered in Ref. [5].

Another dissociation channel in which a phase shift was observed in the interference pattern is known as ground state [13] or vibrational dissociation [10]. There, the dissociation is not caused by an electronic transition to a dissociative state, but rather by an excitation of the nuclear motion to a vibrational continuum state. Disregarding the vibrational state, the molecular ion (H_2^+) remains in the ground state. A π-phase shift was observed in the FDCS for vibrational dissociation following target ionization in 200-eV e^- + H_2 [13] as well as for vibrational dissociation following electron capture in 75-keV p +

H_2 collisions [10]. What is remarkable about these findings is that in these dissociation channels the electronic transition does not lead to a switch in the symmetry of the molecular state. Therefore, the explanation for the phase shift based on parity conservation, which is plausible for dissociation through electronic excitation to an ungerade state, may not hold to explain the observations for vibrational dissociation. However, it has been pointed out that the explanation based on parity conservation cannot be entirely ruled out because apart from the symmetry of the electronic molecular state the one of the state of the nuclear motion (i.e., vibrational and rotational) also needs to be considered [14]. On the other hand, it is not clear why antisymmetric nuclear states would be favored by the collision process.

The data on dissociative capture in p + H_2 collisions were compared to calculations based on two different models. The first one [10,15] represents an ad hoc approach in two regards: first, I_2 is not calculated from first principles, but rather the cross sections for the incoherent case are multiplied by the model interference term reported in Ref. [11]. Second, a phase shift of π was introduced to match the calculated interference pattern with the one observed in experiment. In contrast, the second model [16,17] does not make any assumptions about a π-phase shift. In the calculations of the cross sections as a function of θ_p, the position of the interference extrema at small θ_p is consistent with a phase shift of 0 relative to I2 from Ref. [11]. There, the calculation is not in good agreement with the experimental data. However, at larger θ_p the position of the interference extrema seemed to depart from what is expected for a zero-phase shift and somewhat better agreement with both the experimental data and the calculation based on the first model, assuming a π-phase shift, was obtained. This suggests that in the second model the two-center interference term is more complex than the one reported in Ref. [11]. Parameters which determine the total

phase appear to depend on θ_p. Furthermore, the calculations were performed for fixed values of KER and the results show that the position of the interference extrema depends on that parameter as well.

In our previous experiment reported in Ref. [10] vibrational dissociation was selected by setting a condition on the KER range 0 to 2 eV. However, we neither had sufficient resolution nor statistics to analyze cross sections differential in KER with a narrow bin size. In this paper we report FDCS for fixed KER as a function of θ_p. This was achieved by increasing the number of true vibrational dissociation events by more than an order of magnitude and the momentum resolution of the detected fragments by a factor of 5. The results confirm a significant phase shift compared to the interference term reported in Ref. [11]. Furthermore, the phase shift appears to depend on θp. However, a dependence on KER could not conclusively be identified.

2. EXPERIMENT

The experiment was performed at the medium energy accelerator of the Missouri University of Science & Technology. A proton beam was generated with a hot cathode ion source and accelerated to an energy of 75 keV. The beam was collimated to a size of 0.15 × 0.15 mm2 by a pair of slits placed at a distance of 50 cm from the target chamber. This slit geometry corresponds to a transverse coherence length of about 3.3 a.u. [18]. In the target chamber, the projectile beam was crossed with a very cold (T ∼= 1–2 K) H_2 beam generated with a supersonic gas jet. After the collision the projectiles were charge-state analyzed using a switching magnet. The neutralized beam component was detected by a

two-dimensional position-sensitive microchannel plate detector (MCP). From the position information the azimuthal and polar projectile scattering angles were determined with a resolution of 3◦ and 0.15 mrad full width at half maximum (FWHM), respectively.

The proton fragments from the dissociated target molecule were extracted by a weak electric field of about 7.8 V/cm and traversed a field-free region twice as long as the extraction region in order to achieve optimized time focusing [19]. The fragments were detected by a second two-dimensional position sensitive MCP detector, which was set in coincidence with the projectile detector. The directions of the extraction field (x direction) and of the expansion of the target gas (y direction) define the coordinate system in which the projectile and recoil-ion momenta are analyzed. From the position information, the two momentum components perpendicular to the extraction field (i.e., the y- and z components, where the latter coincides with the projectile beam direction) were determined. The x component of the fragment's momentum $\mathbf{p}_{\mathbf{fr}}$ was obtained from the time of flight from the collision region to the detector, which, in turn, is contained in the coincidence time. From the momentum components the KER and the molecular orientation were calculated.

Compared to our previous experiment [10], the fragment's momentum resolution was significantly improved by two modifications, one in the experimental setup and one in the data analysis: in the experiment the extraction voltage was reduced from 500 to 100 V. In the data analysis, events with a molecular orientation along the x axis were selected. Because the target temperature is negligible in this direction, and due to time focusing, the momentum resolution for the x component is significantly better than for the y component and somewhat better than for the z component. Under these circumstances, the momentum resolution comes mainly from the finite size of the interaction volume, i.e., the overlap

volume between the projectile and target beams, and the time resolution. It is linearly proportional to the extraction voltage. The corresponding resolution in KER depends on the KER itself and ranges from 30-meV FWHM at KER = 0.2 eV to 70-meV FWHM at KER = 1.6 eV. The resolution in the polar and azimuthal angles of the molecular orientation is estimated as 4◦ and 8◦ FWHM, respectively. The azimuthal resolution is worse because ϕ_{fr} depends on the y component of $\mathbf{p_{fr}}$ (i.e., the component with the worst resolution), while θ_{fr} does not.

3. DATA ANALYSIS

Immediately after the collision, the H_2^+ ion moves with a momentum $\mathbf{p_{rec}} = \mathbf{q}$, where **q** is defined as the difference between the initial momentum of the incident proton and the momentum of the scattered neutralized projectile. **q** is related to the momentum transfer from the projectile to the target q by $\mathbf{q} = \mathbf{q'} - \mathbf{v_p}$. Here, the transverse component $q'_{tr} = q_{tr}$ has magnitude $q_{tr} = mv_p\tan\theta_p$ and the longitudinal component of **q** is given by $q_z = (E_f - E_i)/v'_p - v_p/2$, where m and v_p are the mass and velocity of the incident proton, respectively. E_f is the sum of the internal energies of the neutralized projectile and the residual molecular target ion H_2^+ and E_i is the internal energy of the initial target H_2. The recoil momentum $\mathbf{p_{rec}}$ is equally shared by the two atomic centers of the molecule. The dissociation adds a momentum $\mathbf{p_d}$ and $-\mathbf{p_d}$, respectively, to the fragments, measured relative to the center of mass of the molecular ion. As a result, the detected fragment will have a momentum of $\mathbf{p_{fr}} = \mathbf{q}/2 + \mathbf{p_d}$ in the laboratory frame. The molecular orientation of H_2^+ is given by the direction of $\mathbf{p_d}$. Therefore, we subtracted **q**/2 from the measured

momentum $\mathbf{p_{fr}}$ of the charged molecular fragment to obtain the molecular orientation. Since both transverse momentum components of the projectiles are directly measured (using the position information) and the longitudinal component is known from the energy balance, both the magnitude and the direction of **q** are known. The magnitude of **q**/2 ranges from 0.5 a.u. at θ_p = 0.1 mrad to 8 a.u. at θ_p = 5 mrad, while $\mathbf{p_d}$ = 8 a.u. for KER = 1 eV. Therefore, this correction for **q**/2, which was neglected in our previous experiment reported in Ref. [10], is negligible at small, but quite important at large θ_p.

FDCS were analyzed for two molecular orientations. Both of them are perpendicular to the initial projectile beam direction (i.e., $\theta_{mol} = 90^\circ \pm 10^\circ$). One is also perpendicular to the transverse momentum transfer $\mathbf{q_{tr}}$, while the second is parallel to $\mathbf{q_{tr}}$ and we refer to them as the perpendicular and parallel orientations, respectively. As mentioned in the previous section, in both cases molecular orientations along the x axis (within $\pm 10^\circ$) were selected. Therefore, the perpendicular orientation is realized by setting a condition on the azimuthal projectile angle $\phi_p = 90 \pm 10^\circ$ (i.e., scattering in the y direction) and the parallel orientation by setting a condition on $\phi_p = 0^\circ \pm 10^\circ$ (i.e., scattering in the x direction).

For the parallel orientation FDCS were obtained for fixed KERs of 0.2, 0.6, 1.0, and 1.6 eV and plotted as a function of θ_p. Furthermore, data integrated from KER = 0 to 2 eV were analyzed for both orientations and compared to the previously published data [10] which neglected the correction for **q**/2 as well as to theory.

4. RESULTS AND DISCUSSION

In Figure 1 we show the measured cross sections integrated over KER = 0 to 2 eV for the perpendicular (open symbols) and parallel orientations (closed symbols). For the perpendicular orientation no structure can be discerned, but rather the cross sections just drop off monotonically with increasing θ_p. This is the expected behavior because in the two-center interference term

$$I_2 = 1 + \cos(\mathbf{p_{rec}} \cdot \mathbf{D} - \delta) = 1 + \cos(\mathbf{q_{tr}} \cdot \mathbf{D} - \delta), \quad (1)$$

the dot product $\mathbf{q_{tr}} \cdot \mathbf{D}$ is constant at zero for this orientation. δ is a phase shift, which is zero in the original version [11] and yet to be determined for the present case. In contrast, the data for the parallel orientation exhibit a pronounced oscillating pattern with minima at 1.7, 3.8, and 5.7 mrad and maxima at 2.2, 4.5, and 6.8 mrad reflecting the θ_p dependence of $\mathbf{q_{tr}} \cdot \mathbf{D} - \delta$. Note, however, that the oscillating structure is superimposed on very steeply decreasing cross sections, which introduces some uncertainty to the exact location of the interference extrema.

In Figure 2 the data for the parallel orientation of Figure 1 are replotted, but this time in comparison with the corresponding data from Ref. [10] shown as open symbols, which we refer to as the old data. To put this comparison in proper perspective, it should be noted that apart from the $\mathbf{q}/2$ correction another important difference between both data sets lies in the method in extracting the information about the interference pattern. In the new data, it is obtained from a comparison between the coherent FDCS for the parallel and perpendicular orientations (Figure 1), while in the old data it is obtained from a comparison between the coherent and incoherent FDCS for the parallel orientation. For θ_p up to about

1.2 mrad no differences between the two data sets can be discerned, but at larger θ_p the correction for **q**/2 leads to some differences. The main effect of this correction is that the interference structure becomes more pronounced at large θ_p. In fact, in the cross sections of the old data the interference extrema are not fully resolved and only appear as "bumps" in the θ_p dependence. Only in the ratios $R_{\|}$ between the cross sections for coherent and

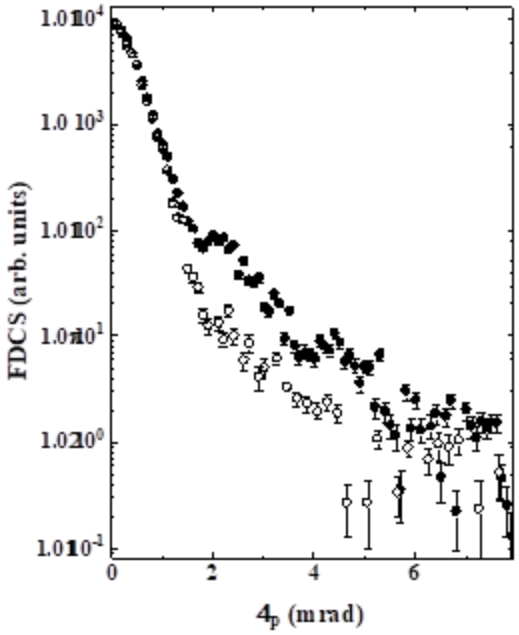

Figure 1. Fully differential cross sections for all KER for perpendicular (open symbols) and parallel (closed symbols) molecular orientations as a function of projectile scattering angle.

incoherent projectiles a clear oscillating pattern was observed. The positions of the interference extrema in these ratios are generally shifted to slightly smaller θ_p compared to those seen in the cross sections of the present data.

The $R_{\|}$ for the old data were fairly flat up to about θ_p = 0.8 mrad. This ratio was thought to represent a product of the interference terms for two-center molecular and single-center interference I1 [20]. The latter was obtained from the coherent and incoherent cross sections for the perpendicular plane, for which I_2 was assumed to be constant. I_2 was

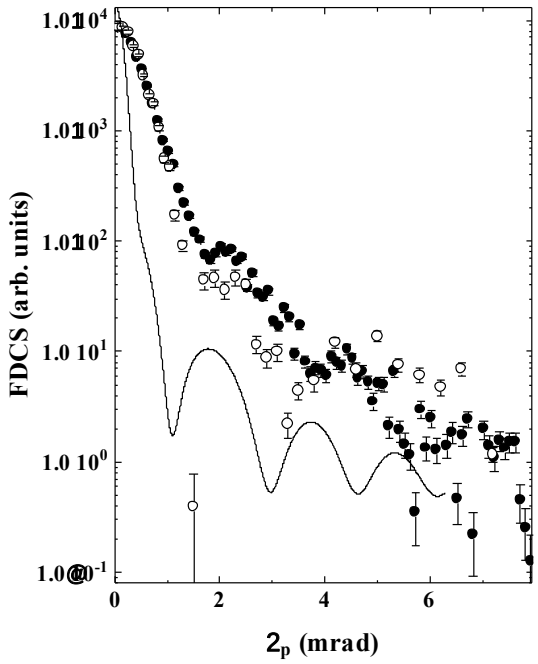

Figure 2. The data of Figure 1 for the parallel orientation replotted in comparison to the data of Lamichhane et al. The solid curve shows our calculation.

then extracted as a double ratio between R|| and I1. It showed a pronounced minimum at θp = 0, which was taken as a first hint that I2 is afflicted with a π-phase shift. This analysis has to be reconsidered based on the present data.

In the new experiment, one important objective was to optimize the recoil-ion momentum resolution. This precluded measuring the cross sections for coherent and incoherent projectile beams simultaneously, as was done in Ref. [10]. This would require

obtaining either the coherent or the incoherent data for molecular fragments ejected in the y direction, for which the recoil momentum resolution is significantly worse than for the x direction. On the other hand, it should be possible to isolate I_2 as a ratio between the coherent cross sections for the parallel and perpendicular orientations under the assumption that the incoherent part of the cross section is independent of the molecular orientation. However, Figure 1 strongly suggests that this assumption is not justified for θ_p larger than

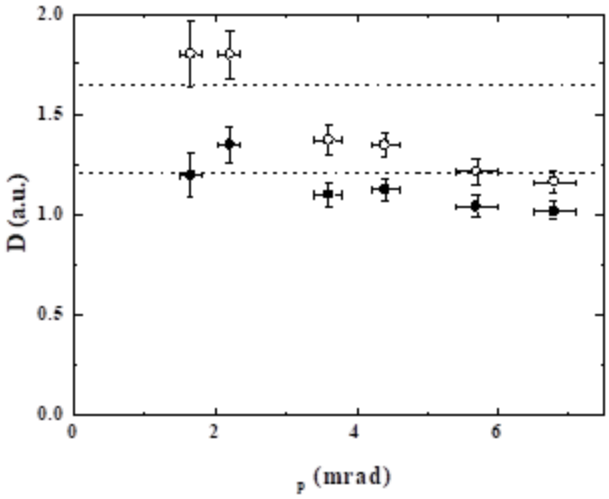

Figure 3. Internuclear distance **D** of the molecule at the instant of the transition extracted from the location of the interference extrema under the assumption that there is no phase shift in the interference term (open symbols) or a phase shift of π (closed symbols).

about 1.5 mrad, where the data for the perpendicular orientation are systematically smaller than for the parallel orientation by a large factor. The assumption may be valid for smaller θ_p, where the two data sets nearly coincide. If it is, then the similarity between the cross sections for both orientations in this region suggests that here, interference effects are weak.

Since no interference pattern is discernible for small θ_p, the behavior at $\theta_p = 0$ obviously cannot be used to make any conclusions about the phase shift δ in I_2. In the following, we, therefore, attempt to gain that information from the location of the interference extrema observed for θ_p>1 mrad. According to Eq. (1) the extrema occur when $\mathbf{q} \cdot \mathbf{D} - \delta = n\pi$, which for the parallel orientation becomes $mvp \tan \theta_p \mathbf{D} - \delta = n\pi$. This relation is not sufficient to determine both **D** and δ at the same time. We therefore first determine an average value of **D** under the assumption that δ is either 0 or π as a function of θ_p. These data are shown in Figure 3 as open ($\delta = 0$) and closed symbols ($\delta = \pi$), respectively. The horizontal dashed lines indicate the location of the classical inner and outer turning points for the ground-state vibration of H2. At small θp the data favor $\delta = \pi$ as the assumption $\delta = 0$ results in D larger than the location of the outer turning point. Likewise, at large θp the assumption $\delta = \pi$ results in D smaller than the location of the inner turning point. A value of D close to the inner turning point is consistently obtained if δ is assumed to evolve from around π at θp = 1.5 mrad to around 0 for θp>5 mrad. Such a dependence of δ on θp is indeed found if δ is calculated under the assumption D = 1.2 a.u., the location of the inner turning point [21], which is plotted in Figure 4. Indeed, vibrational dissociation is expected to strongly favor the inner turning point [22] because of the maximized overlap between the nuclear wave functions for the initial and final vibrational states.

It is not unreasonable to assume that for the perpendicular orientation δ depends on θ_p as well (although one would not necessarily expect the same dependence as for the parallel orientation). If that is the case then even for this orientation, despite the constant $\mathbf{q_{tr}} \cdot \mathbf{D}$, an interference structure would be expected. However, the oscillation length would

probably be considerably longer than for the parallel orientation. For example, the period of oscillation for the parallel orientation due to $\delta(\theta_p)$ alone (i.e., ignoring $\mathbf{q_{tr}} \cdot \mathbf{D}$) would be about 8 mrad according to Figure 4. An oscillation with such a long period, superimposed on steeply decreasing incoherent cross sections, may be difficult to identify, especially at large θ_p, where the statistical errors are relatively large. Nevertheless, Figure 1 shows that

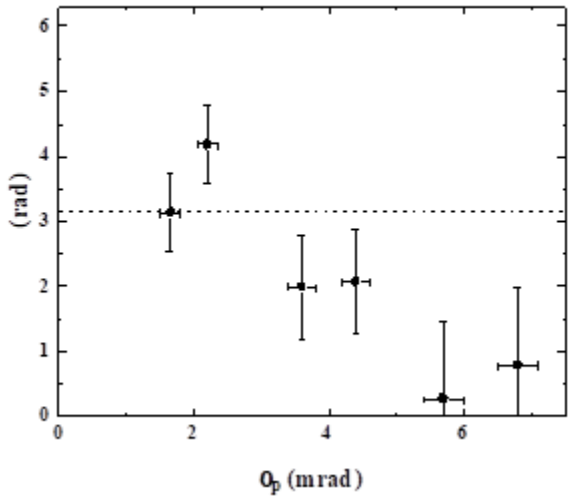

Figure 4. Phase-shift δ in the interference term extracted from the location of the interference extrema under the assumption that the transition always occurs at the classical inner turning point of the initial vibrational state.

the cross sections for the perpendicular orientations significantly drop below those for the parallel orientation between θp = 1.5 and 5 mrad and the two data sets then approach each other again at very large θp. This might be a signature of a large-period interference oscillation.

The solid lines in Figure 2 show our theoretical calculations based on a distorted wave approach. The details of this model were published previously [16,17]. In short, the

transition amplitude is obtained within an impact parameter formulation and includes the interaction between the projectile and each nucleus of the molecule Vnn. Vibrational dissociation is accounted for by convoluting the spatial part of the transition amplitude with the overlap between the initial and final vibrational states. The θ_p-dependent transition amplitude is then obtained as a Fourier transform of the impact parameter dependent amplitude.

As in the experimental data, the FDCS were integrated over KER from 0 to 2 eV. As in the experimental data, the calculation, too, exhibits a pronounced oscillatory structure with minima at 1.07, 2.9, 4.6, and 6.1 mrad and maxima at 1.8, 3.7, and 5.3 mrad. Thus, the oscillation length, ranging between 1.5 and 1.9 mrad, depending on θp, is somewhat smaller than in the experimental data (1.9–2.3 mrad). However, the location of the interference extrema is quite sensitive to the oscillation length and this leads to significant discrepancies between theory and experiment. Furthermore, the θp dependence of the theoretical cross sections is much steeper compared to the measured cross sections. This could be indicative for an underestimation of the importance of Vnn, which is expected to have a particularly large effect at large θ_p.

The discussion of the FDCS integrated over KER = 0 to 2 eV strongly suggests that the phase-shift δ depends on θ_p. In the following we will investigate whether δ also depends on the KER. To this end, the FDCS for the parallel orientation are plotted for fixed KER, as indicated in the insets, as a function of θ_p in Figure 5. Interference extrema are observed at about the same θ_p as in the FDCS integrated over KER, although at large θ_p the lower statistics makes an accurate determination of the location of the extrema difficult. Furthermore, we cannot identify any difference in the location of the extrema between the

FDCS for the various KER. This shows that δ has a much weaker, if any, dependence on KER than on θ_p. Contrary to the experimental data, the calculation (solid lines in Figure 5) shows a significant dependence of the location of the interference extrema on KER. In Figure 6 the calculations for the various KER are compared and it can be seen that with increasing KER the interference extrema systematically move to larger θ_p. As a result, the agreement between experiment and theory tends to be somewhat better at large KER than at small KER.

The experimental observations and the comparison to theory raise several questions:

(a) Why is the interference term afflicted with a nonzero phase shift although the molecular transition does not involve a change of symmetry?

(b) Why does the phase shift depend on θ_p, but not on KER?

(c) Why is the interference structure not visible for $\theta p<1.5$ mrad?

(d) Why are the dependencies of the interference term on θp and KER so different between experiment and theory?

In the following we will offer a hypothetical explanation addressing these questions, for which, however, we cannot yet provide conclusive evidence. It is based on a classical analogy. It is well known that mechanical waves reflected from a fixed end suffer a phase leap of π. The quantum-mechanical equivalent is reflection of a particle wave from a potential wall of infinite height. Such a scenario is approximately realized in nuclear excitation to a vibrational continuum state. Although the potential does not step up sharply at a well-defined location to infinity, as for a potential wall, the potential-energy curves of the molecular states do rise very steeply as **D** decreases and asymptotically go to infinity.

Therefore, if the vibrational wave packet propagates towards decreasing immediately after the transition, one would expect a reflection of the wave packet near the inner turning point with a π-phase leap resulting in dissociation as the reflected wave packet

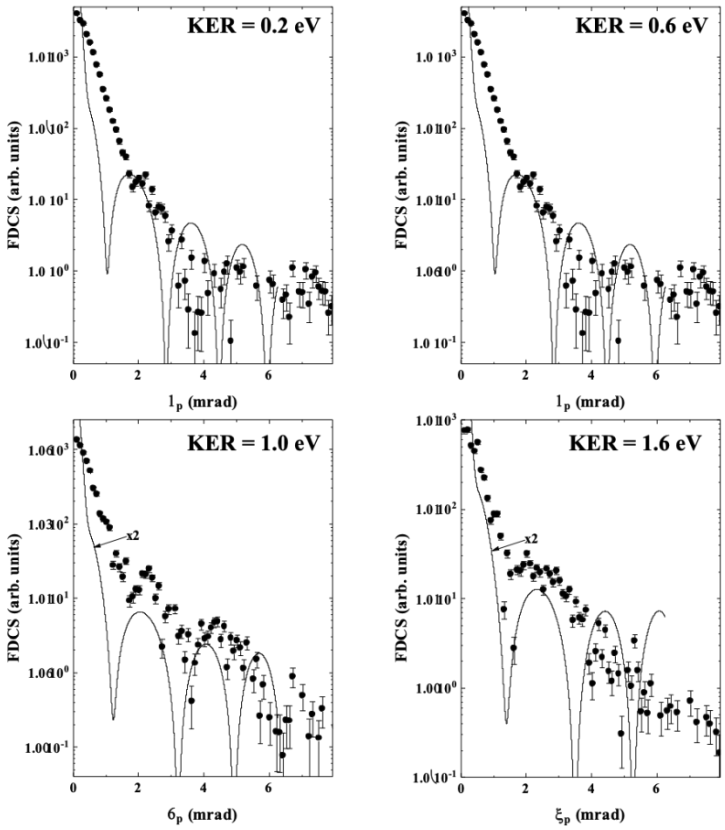

Figure 5. Fully differential cross sections for the parallel molecular orientation for various fixed values of KER (see insets) as a function of projectile scattering angle. The solid lines show our calculations.

propagates towards increasing **D**. While reflection of the vibrational wave packet preceding dissociation is generally possible, it obviously is not a prerequisite for dissociation. In a direct path, where the wave packet immediately propagates towards increasing **D**, no

reflection occurs, and one would consequently not expect any phase leap. In the experiment, it cannot be distinguished whether dissociation proceeds through the direct or

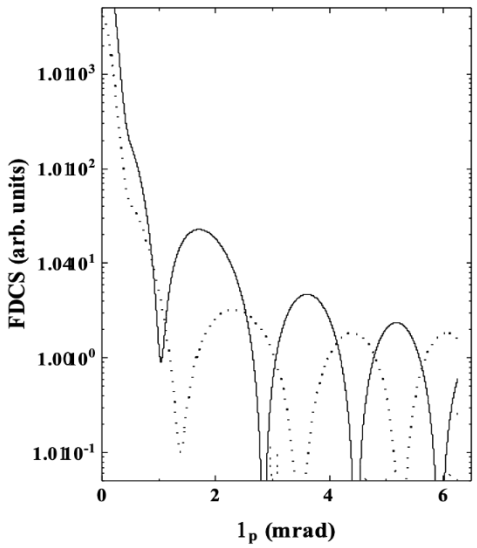

Figure 6. Comparison of the theoretical fully differential cross sections for the KER values of Fig. 5 to illustrate the dependence of the location of the interference extrema on the KER. Solid curve, KER = 0.2 eV; dashed curve, KER = 0.6 eV; dashed-dotted curve, KER = 1.0 eV; dotted curve, KER = 1.6 eV.

the reflection path and each may occur with some probability. The cross sections would then reflect a combination of the interference terms with and without π-phase shift. Equal probabilities would then result in a vanishing interference term. Likewise, an interference structure with phase shift would be indicative of a dominant reflection path and one without phase shift would be indicative of a dominant direct path.

Based on these arguments the data of Figure 4 suggest that the reflection path is favored at small θ_p (but not smaller than 1.5 mrad) and the direct path at large θ_p. This

dependence of δ on θ_p can be understood within a classical picture. If the impact parameter b (relative to the center of mass of the molecule) is smaller than **D**/2 at the instance of the transition, then the projectile will exert a repulsive force on both protons of the molecule driving them apart (corresponding to the direct path). If, on the other hand b is larger than **D**/2, both molecular protons are repelled in the same direction by the projectile. However, the strength of the force will be larger on the proton which is closer to the projectile, resulting in a tidal force which will push the two protons closer together (corresponding to the reflection path). Since small b are more selective on large θ_p and large b on small θ_p this could explain the dependence of δ on θ_p observed in Figure 4. The magnitude of the tidal force maximizes at b = **D**/2 and goes asymptotically to zero for b approaching infinity. Therefore, for very small θ_p the effect of the tidal force pushing both protons closer together becomes negligible. In this case, the interaction of the projectile with the molecular protons merely displaces the center of mass of the molecule, but it does not significantly affect the relative motion between the two protons. This scenario favors neither the direct nor the reflection path, which would explain the vanishing of the interference structure observed in the experimental data for θ_p<1.5 mrad.

The observation that the phase shift does not depend on the KER is not surprising. In contrast to dissociation through electronic excitation, in vibrational dissociation there is not a strong correlation between the KER and **D**. All vibrational continuum states are accessible in the entire Franck-Condon region of the ground state of H_2. At the same time, the total energy of the molecule is constant for each vibrational state, i.e., it does not depend on **D** within the Franck-Condon region. Therefore, one would expect **D** corresponding to the inner turning point to be favored regardless of the KER due to the maximized overlap

between the initial and final vibrational state wave functions. However, the observed independence of the location of the interference extrema on the KER appears to be in conflict with our calculations, in which we find a significant dependence on the KER. At present, we do not have an explanation for this difference between the experimental data and the calculations and further studies are called for.

5. CONCLUSIONS

We have presented a joint experimental and theoretical study on vibrational dissociation following electron capture in 75-keV p + H_2 collisions. The complete kinematic information of all collision fragments in the final state was determined, from which fully differential cross sections FDCS were extracted. Our analysis focuses on a molecular orientation perpendicular to the initial projectile beam axis and parallel to the transverse momentum transfer. A pronounced two-center molecular interference structure was observed in both the experimental data and in the calculated FDCS as a function of projectile scattering angle θ_p. However, there are significant discrepancies between the measured and calculated data.

Previously we reported on data for the same process and the same kinematics but integrated over the entire KER region in which vibrational dissociation can occur [10]. There, we found a phase shift which was thought to be constant at π for all θ_p. A more detailed analysis of the new data suggests that the phase shift actually varies between π at relatively small θ_p and nearly 0 at large θ_p. The FDCS for fixed KER exhibit interference extrema at about the same locations as in the cross sections integrated over KER. This

suggests that the phase shift is (nearly) independent of the KER. In contrast, in our calculations the locations of the interference extrema significantly depend on the KER.

We have presented a hypothetical explanation for these observations. It assumes that the vibrational wave packet can either propagate towards larger internuclear distances, which results in direct dissociation because the molecule is in a vibrational continuum state, or towards smaller internuclear distances. In this case the wave packet has to be reflected at the inner turning point before dissociation can occur. Such a reflection from a steep potential wall results in a phase leap manifesting itself in a corresponding phase shift in the interference term. Within a classical picture we argued that relatively small (but not too small) θ_p should favor the reflection path and large θp the direct path. Within our model both paths should occur with similar probabilities for very small θ_p . This would explain the vanishing of the interference structures at these very small scattering angles. However, we emphasize that we do not claim ultimate evidence for the correctness of our model. Rather, we hope that it will trigger further theoretical studies to either confirm or dismiss our explanation for the phase shift.

We further emphasize that if our model is confirmed the explanation for the phase shift is qualitatively different from the reason for a similar (but constant) phase shift observed in dissociation following electronic excitation to an antisymmetric dissociative state, where the explanation is based on parity conservation [5].

ACKNOWLEDGEMENTS

This work was supported by the National Science Foundation under Grant No. PHY-2011307. Valuable discussions with Dr. Raul Barrachina and Dr. Marcelo Ciappina are gratefully acknowledged.

REFERENCES

[1] T. F. Tuan and E. Gerjuoy, Phys. Rev. 117, 756 (1960).

[2] S. Cheng, C. L. Cocke, V. Frohne, E. Y. Kamber, J. H. McGuire, and Y. Wang, Phys. Rev.A 47, 3923 (1993).

[3] N. Stolterfoht, B. Sulik, V. Hoffmann, B. Skogvall, J. Y. Chesnel, J. Rangama, F. Frémont, D. Hennecart, A. Cassimi, X. Husson, A. L. Landers, J. A. Tanis, M. E. Galassi, and R. D. Rivarola, Phys. Rev. Lett. 87, 023201 (2001).

[4] D. Misra, U. Kadhane, Y. P. Singh, L. C. Tribedi, P. D. Fainstein, and P. Richard, Phys. Rev. Lett. 92, 153201 (2004).

[5] L. Ph. H. Schmidt, S. Schössler, F. Afaneh, M. Schöffler, K. E. Stiebing, H. Schmidt Böcking, and R. Dörner, Phys. Rev. Lett. 101, 173202 (2008).

[6] H. T. Schmidt, D. Fischer, Z. Berenyi, C. L. Cocke, M. Gudmundsson, N. Haag, H. A. B. Johansson, A. Källberg, S. B. Levin, P. Reinhed, U. Sassenberg, R. Schuch, A. Simonsson, K. Støchkel, and H. Cederquist, Phys. Rev. Lett. 101, 083201 (2008).

[7] J. S. Alexander, A. C. Laforge, A. Hasan, Z. S. Machavariani, M. F. Ciappina, R. D. Rivarola, D. H. Madison, and M. Schulz, Phys. Rev. A 78, 060701(R) (2008).

[8] L. Ph. H. Schmidt, T. Jahnke, A. Czasch, M. Schöffler, H. Schmidt-Böcking, and R. Dörner, Phys. Rev. Lett. 108, 073202 (2012).

[9] S. F. Zhang, D. Fischer, M. Schulz, A. B. Voitkiv, A. Senftleben, A. Dorn, J. Ullrich, X. Ma, and R. Moshammer, Phys. Rev. Lett. 112, 023201 (2014)

[10] B. R. Lamichhane, T. Arthanayaka, J. Remolina, A. Hasan, M. F. Ciappina, F. Navarrete, R. O. Barrachina, R. A. Lomsadze, and M. Schulz, Phys. Rev. Lett. 119, 083402 (2017).

[11] A. Messiah, in Quantum Mechanics (North-Holland, Amsterdam, 1970), Vol. II, pp. 848852.

[12] B. R. Lamichhane, A. Hasan, T. Arthanayaka, M. Dhital, K. Koirala, T. Voss, R. A. Lomsadze, and M. Schulz, Phys. Rev. A 96, 042708 (2017).

[13] A. Senftleben, T. Pflüger, X. Ren, O. Al-Hagan, B. Najjari, D. Madison, A. Dorn, and J. Ullrich, J. Phys. B 43, 081002 (2010).

[14] R. Barrachina, private communication (2019).

[15] M. F. Ciappina, O. A. Fojon, and R. D. Rivarola, J. Phys. B 47, 042001 (2014).

[16] A. Igarashi and L. Gulyas, J. Phys. B 52, 075204 (2019). [17] A. Igarashi, J. Phys. B 53, 225205 (2020).

[17] A. Igarashi, J. Phys. B 53, 225205 (2020)

[18] K. N. Egodapitiya, S. Sharma, A. Hasan, A. C. Laforge, D. H. Madison, R. Moshammer, and M. Schulz, Phys. Rev. Lett. 106, 153202 (2011).

[19] W. C. Wiley and I. H. McLaren, Rev. Sci. Instrum. 26, 1150 (1955).

[20] T. P. Arthanayaka, S. Sharma, B. R. Lamichhane, A. Hasan, J. Remolina, S. Gurung, and M. Schulz, J. Phys. B 48, 071001 (2015).

[21] T. E. Sharp, Atomic Data 2, 119 (1971).

[22] A. Senftleben, T. Pflüger, X. Ren, B. Najjari, A. Dorn, and J. Ullrich, J. Phys. B 45, 021001(2012).

II. INTERFERENCE BETWEEN FIRST- AND HIGHER-ORDER IONIZATION AMPLITUDES NEAR THE VELOCITY MATCHING IN 75 KeV p + He COLLISIONS

S. Bastola[1], M. Dhital[1,2], S. Majumdar[1], A. Hasan[3], R. Lomsadze[4], J. Davis[1], S. Borbély[5], L. Nagy[5], and M. Schulz[1]

[1]Physics Dept. and LAMOR, Missouri University of Science & Technology, Rolla, MO 65409, USA

[2]Physics Dept., University of California-Riverside, Riverside, CA 92521, USA

[3]Dept. of Physics, UAE University, P.O. Box 15551, Al Ain, Abu Dhabi, UAE

[4]Dept. of Exact and Natural Science, Tbilisi State University, Tbilisi 0179, Georgia

[5]Faculty of Physics, Babeș-Bolyai University, Kogălniceanu St. 1, 400084 Cluj, Romania

ABSTRACT

We have measured and calculated fully differential cross sections for ionization of He by 75 keV p impact for a small projectile coherence length close to the size of the target atom. Data were taken for an ejected electron energy corresponding to a speed close to the projectile speed (velocity matching). In the fully differential angular electron distributions, a pronounced double-peak structure, observed previously for a coherence length much larger than the atomic size, is much less pronounced in the current data. This observation is interpreted in terms of interference between first- and higher-order transition amplitudes. Although there are significant quantitative discrepancies between experiment and theory, the qualitative agreement supports this interpretation.

1. INTRODUCTION

One of the most important goals of atomic collision research is to advance our understanding of the fundamentally important few-body problem (FBP) [e.g. 1,2]. The essence of the FBP is that the Schrödinger equation is not solvable in closed form for more than two mutually interacting particles, even when the underlying forces are precisely known. Theoretically, the FBP in atomic collisions has been tackled by perturbative [e.g. 2-10] and, more recently, by non-perturbative [e.g. 1,11-15] approaches. In treatments employing the Born series understanding the few-body dynamics of the collision basically means accurately describing the relative contributions of the leading-order process to the various higher-order processes to the cross sections. In contrast, in distorted wave and non-perturbative methods these contributions usually don't occur as separate terms in the transition amplitude (as they do in the Born series). There, the accuracy of the description of higher-order processes depends on how well the exact final-state wavefunction of the collision system is approximated (distorted wave methods) or on the size of the basis set and on the appropriate selection of the basis states (non-perturbative methods).

Here, our interest is focused on ionization of the target by ion-impact. There, one higher-order mechanism that has been studied extensively is known as post-collision interaction (PCI) [e.g. 16-25]. PCI involves at least two interactions between the projectile and the active target electron. In the first interaction the projectile transfers sufficient energy for the electron to be lifted to the continuum. In the second interaction the ejected electron and the projectile attract each other in the outgoing part of the collision towards the initial beam axis. Because of momentum conservation the residual target ion needs to

be involved as well, i.e. momentum exchange must occur between the recoil ion and either the electron or the projectile [22]. PCI is particularly prominent for electrons ejected with an energy corresponding to a speed close to the projectile speed (velocity matching). Pronounced signatures of PCI have been observed in ejected electron spectra [e.g. 16,17,19,21], in recoil-ion momentum spectra [20], and in scattered projectile spectra [18,22,25].

The most detailed information about the reaction dynamics in atomic collisions can be extracted from fully differential cross sections (FDCS) measured in kinematically complete experiments (for reviews see [26-28]). If the first-order mechanism is the dominant contribution to the FDCS the angular ejected electron distribution exhibits a characteristic double-peak structure, with the binary peak occurring in the direction of the momentum transfer **q** and the recoil peak in the direction of **–q** [e.g. 2,29]. However, for slow and/or highly-charged ion impact, these structures are shifted in the forward direction relative to **q** or **–q**, respectively, due to PCI [e.g. 30-34] (often, the recoil peak disappears altogether). If the ejected electron energy corresponds to the velocity matching region, another signature of PCI is observed: it then leads to a pronounced peak structure occurring in the initial projectile beam direction (forward peak), which at large scattering angles θ_p is separated from the binary peak by a minimum [23,35,36]. The forward peak can be understood in terms of a mutual focusing effect between the projectile and the ejected electron in the outgoing part of the collision. For electron impact such a focusing does not occur because of the repulsive nature of the interaction between the projectile and the target electron. Therefore, the forward peak can only be studied in collisions of either ions or positrons with atoms or molecules.

At first glance, separate forward and binary peak structures may appear plausible, at least if the binary peak is basically viewed as a signature of the first-order process and the forward peak as a signature of PCI. Because of momentum conservation the binary peak is then expected near the direction of **q** and the forward peak, due to the focusing effect caused by PCI, at 0^o. However, as stated in the previous paragraph, the binary peak cannot entirely be attributed to the first-order process, but rather the forward shift is a signature of PCI as well. The existence of the forward peak and the shift of the binary peak are then just two different manifestations of the same mechanism, which only differ quantitatively in the shift relative to **q**. This raises the question why a relatively small shift (binary peak) and a large shift (forward peak) are very likely, but an intermediate shift (minimum separating both peaks) is less likely. Classically, one would expect a single peak with a centroid somewhere between the direction of **q** and 0^o with a wing on the small-angle side extending towards 0^o. However, in quantum-mechanics a possible explanation for the double peak structure is based on interference between the first-order and higher-order amplitudes.

For interference to be observable experimentally, the incoming projectile must be coherent [37,38]. The importance of such projectile coherence effects has been confirmed by theory [e.g. 39-41]. The transverse coherence length Δx, in turn, can be manipulated, like in classical optics, in terms of a collimating slit placed before the target [37,38]. For a given slit width, Δx then increases with increasing slit distance from the target. Our previous studies, reporting a double forward/binary peak structure [35,36], were performed for a relatively large slit distance, corresponding to Δx larger than 3 a.u. Here, we report on a measurement with $\Delta x < 1$ a.u. under otherwise identical conditions. Indeed, the double

peak structure is found to be much less pronounced, if present at all, for the smaller coherence length. This supports the interpretation that the double peak structure is caused by interference between the first- and higher-order transition amplitudes. This finding is qualitatively also backed by our calculations.

2. EXPERIMENT

The experiment was performed at the medium-energy accelerator of the Missouri University of Science and Technology. A schematic sketch of the set-up is shown in Figure 1. A proton beam with an energy spread of much less than 1 eV was generated with a hot-cathode ion source and accelerated to an energy of 75 keV using a high-voltage platform. The beam was collimated by a pair of slits with a width of 150 μm before entering the target chamber. The vertical slit (collimation in x-direction) was placed at a distance of 7 cm from the target and the horizontal slit (collimation in y-direction) at a distance of 50 cm. The slit geometry for the horizontal slit corresponds to a transverse coherence length Δy of more than 3 a.u. The collimating slit can only increase, but not decrease the coherence length compared to an uncollimated beam. In the x-direction the vertical slit would lead to a transverse coherence length of 0.5 a.u. if the uncollimated beam was completely incoherent. However, because of apertures in the accelerator terminal the actual transverse coherence length in the x-direction is $\Delta x \approx 1$ a.u. In the longitudinal direction the coherence length is determined by the intrinsic energy spread of the projectiles. Since the intrinsic energy spread cannot be larger than the total energy spread, corresponding to a momentum uncertainty of 0.02 a.u., the latter provides a lower limit for

the longitudinal coherence Δz of about 50 a.u. Therefore, the beam can be regarded as longitudinally coherent.

In the target chamber the projectile beam was crossed with a very cold (T ≈ 1-2 K) atomic He beam from a supersonic gas jet propagating in the vertical direction. The scattered protons which did not charge exchange were selected with a switching magnet and decelerated to an energy of 5 keV using another high-voltage platform. The projectiles were then energy-analyzed with an

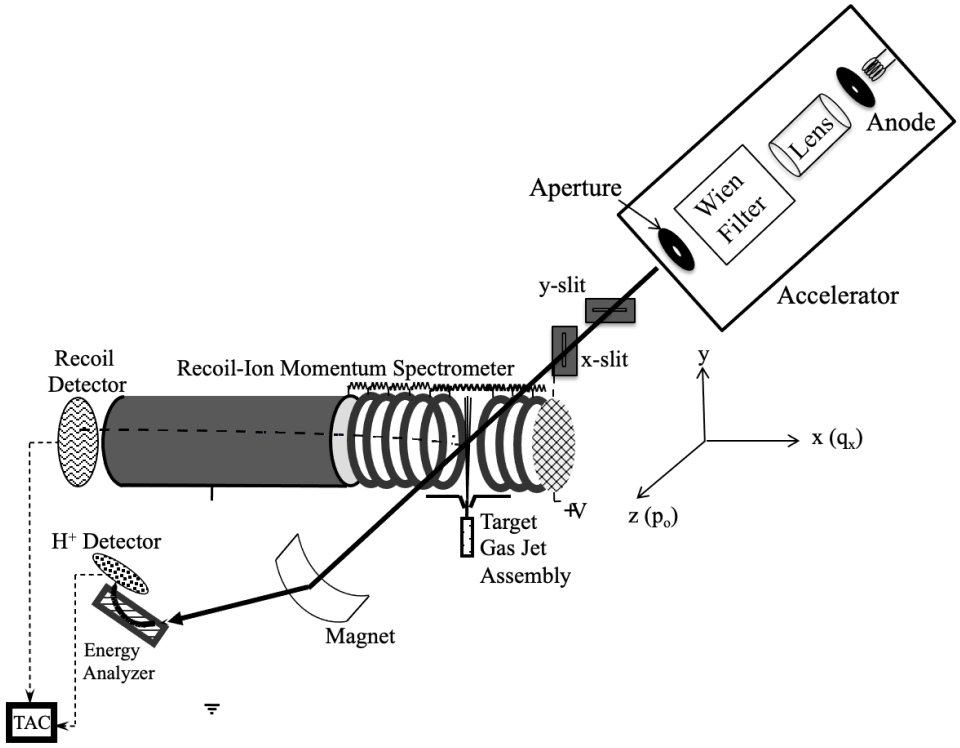

Figure 1. Schematic sketch of the experimental set-up

electrostatic parallel-plate analyzer [42] and detected with a two-dimensional position sensitive micro-channel plate detector (MCP). The entrance and exit slits of the analyzer

had a length of several cm in the horizontal (x-direction) and a width of 75 μm in the vertical direction (y-direction). The analyzer was set to a pass energy corresponding to an energy loss of $\varepsilon = 68.5$ eV with a resolution of 2.5 eV full width at half maximum (FWHM). From ε the longitudinal component and from the position the x-component of the scattered projectile momentum were determined. Due to the narrow width of the slits the y-component was fixed at 0 and the projectile transverse coherence properties are primarily determined by Δx. The momentum transfer is defined by $\mathbf{q} = \mathbf{p_o} - \mathbf{p_f}$, where $\mathbf{p_o}$ and $\mathbf{p_f}$ are the initial and final projectile momenta, and θ_p is determined by $\tan \theta_p = q_x/p_o$. The resolution in θ_p was 0.12 mrad FWHM.

The recoiling target ions were extracted in the x-direction with a weak electric field of 6 V/cm and then traversed a field-free region twice as long as the extraction region. The recoil ions were detected with a second two-dimensional position-sensitive detector, which was set in coincidence with the projectile detector. From the position information the recoil-ion momentum components in the y- and z-direction (defined by the initial projectile beam direction) were determined, and the x-component was obtained from the coincidence time. The ejected electron momentum is then calculated from momentum conservation as $\mathbf{p_{el}} = \mathbf{q} - \mathbf{p_{rec}}$, i.e. the data are kinematically complete. The momentum resolution for the x- and y-components was about 0.15 a.u. FWHM. In the y-direction the resolution is significantly worse ($\approx$ 0.35 a.u. FWHM). However, here our interest is focused on electrons ejected into the scattering plane spanned by the initial and final projectile momenta (i.e. the xz-plane). The recoil-ion resolution in the y-direction causes some uncertainty in the definition of the scattering plane in the data analysis, but it does not affect the polar angular resolution of the electrons ejected into that plane. The resolution in the

azimuthal electron angle φ_{el} (defining the emission plane) was about 20^o FWHM. The resolution in the polar angle θ_{el} depends on θ_{el} itself and ranged from 8^o to 12^o.

3. THEORY

The theoretical model of ionization by charged particle impact for calculating the FDCS as a function of the coherence width of the wave packet associated to the projectile was described in detail elsewhere [40,43]. Briefly, as a first step the impact-parameter dependent transition probability amplitude $a(\mathbf{b}, E, \Omega_e)$ is calculated *ab-initio*, E being the energy and Ω_e the ejection angle of the electron. We numerically solve the time-dependent Schrödinger equation for the two active electrons of the target, which are moving in the combined electric field of the target core and of the projectile [13,44]. The angular part of the electronic wave function was represented in the basis of coupled symmetrized spherical harmonics [13] centered on the target, while the radial partial waves were discretized using the finite element discrete variable representation method [45]. For the time-propagation of the wave function the short iterative Lanczos method [46] with adaptive time-step size control was used.

For a given impact parameter, the transition amplitudes were extracted by projecting the time dependent wave function onto single continuum eigenstates. We have approximated these eigenstates as a symmetrized product of single electron He^+ bound states and Coulomb continuum states. This approach was successfully applied to describe the electronic dynamics induced by negatively charged projectiles in He [13, 47], however in the case of positively charged projectiles it has some shortcomings due to the presence

of the capture channel. The corresponding bound projectile states are poorly represented in a target-centered basis set, and they are not orthogonal to the uncorrelated single continuum eigenstates used in the calculation of the transition probability amplitudes. These two factors have an impact on the predicted transition amplitudes and thus on the predicted FDCS.

In case of the coherent calculation, we associate a plane wave to the projectile (implying infinite transverse coherence length), and the scattering amplitude depending on the transverse momentum transfer $\mathbf{q}_\perp$ may be obtained from an inverse Fourier transform of the probability amplitude [48]

$$R_c(\mathbf{q}_\perp, E, \Omega_e) = \frac{1}{2\pi}\int d^2\mathbf{b} e^{i\mathbf{b}\cdot\mathbf{q}_\perp} b^{2i\frac{Z_p Z_T}{v_p}} a(\mathbf{b}, E, \Omega_e).$$

Here $b^{2i\frac{Z_p Z_T}{v_p}}$ is an eikonal factor accounting for the projectile-nucleus interaction, Z_p and Z_T being the charges of the two particles and v_p the velocity of the projectile.

In our model the finite coherence width of the wave packet of the projectile is taken into account by multiplying the transition probability amplitude by a two-dimensional Gaussian

$$R(\mathbf{q}_\perp, E, \Omega_e) = \frac{N}{2\pi}\int d^2\mathbf{b} e^{i\mathbf{b}\cdot\mathbf{q}_\perp} b^{2i\frac{Z_p Z_T}{v_p}} a(\mathbf{b}, E, \Omega_e) e^{-\frac{(b_x - b_{0x})^2}{2\sigma_x^2} - \frac{(b_y - b_{0y})^2}{2\sigma_y^2}}.$$

Here $\{b_x, b_y\}$ are the components of the impact parameter $\mathbf{b}$, while σ_x and σ_y stand for the standard deviations. x is parallel to $\mathbf{q}_\perp$ and y is perpendicular to $\mathbf{q}_\perp$ and to the initial trajectory of the projectile. The coherence width of the projectile in each direction is considered to be the full width at half maximum (FWHM) of the Gaussian $\Delta b_{x,y} = 2.355\ \sigma_{x,y}$.

Because the center of the wave packet is considered to be on the x axis, $b_{0y} = 0$, while b_{0x} is calculated on the basis of classical scattering of the projectile off the residual ion He^+. It should be noted, however, that the inverse Fourier transform integrates over all impact parameters contributing to each scattering angle for a given coherence length. Therefore, only for a completely incoherent case (i.e., a coherence length of 0) our treatment implies classical projectile trajectories. A finite coherence length, in contrast, corresponds to an uncertainty in the relation between impact parameter and scattering angle. The normalization factor *N* is obtained by normalizing the cross section integrated over the electron ejection angles obtained with a finite coherence width to the coherent results.

Finally, the FDCS is obtained from the scattering amplitude

$$\frac{d^3\sigma}{dEd\Omega_e d\mathbf{q}_\perp} = p_0 |R(\mathbf{q}_\perp, E, \Omega_e)|^2,$$

p_0 being the projectile's initial momentum.

4. RESULTS AND DISCUSSION

From the kinematically complete data we extracted FDCS for electron ejection into the scattering plane for various fixed θ_p as a function of θ_{el}. The fixed energy loss is equivalent to an electron energy of $E_{el} = \varepsilon - I = 43.9$ eV, where I is the ionization potential of He, corresponding to an electron to projectile speed ratio of 1.04. In Figure 2 the FDCS are shown for $\theta_p = 0.1$, 0.2, 0.3, and 0.5 mrad (as indicated in the insets). The open symbols represent data taken for the large slit distance and reported in [36] and the closed symbols

show the present data taken for a small slit distance. For simplicity, we refer to these data as coherent or incoherent, respectively. However, it should be noted that the data are neither completely coherent nor completely incoherent, which would require coherence lengths of infinity or zero, respectively. Here, the terms coherent and incoherent refer to the larger or smaller of the two transverse coherence lengths.

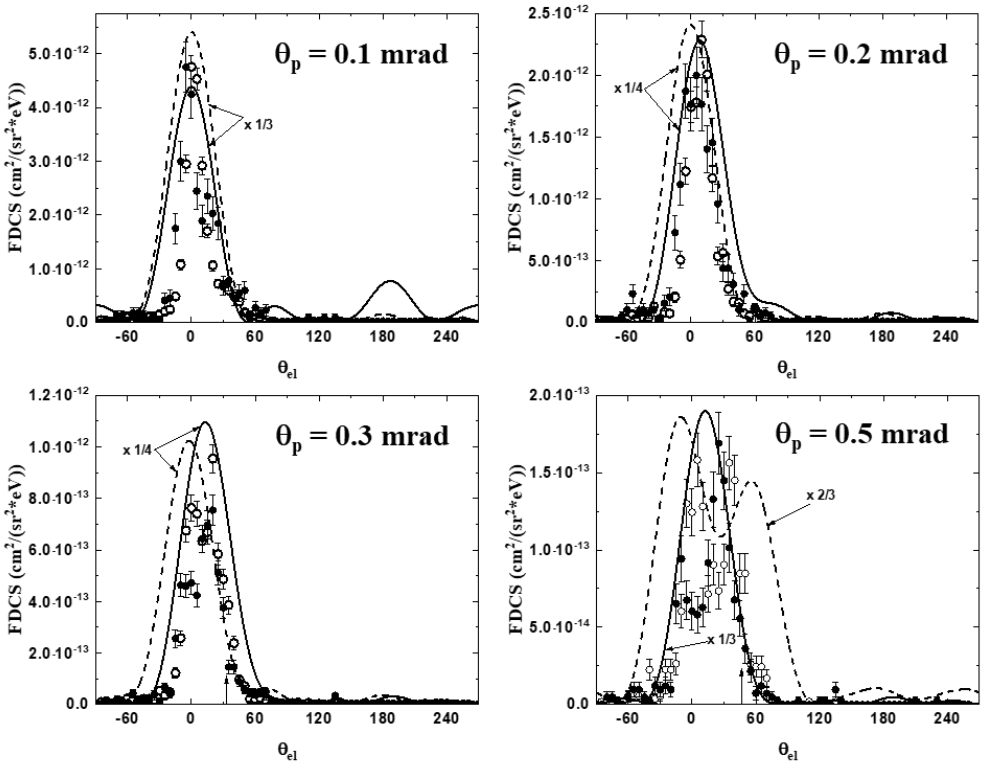

Figure 2. FDCS for electrons ejected into the scattering plane for fixed θ_p as indicated in the insets as a function of θ_{el}. Open symbols, coherent data; closed symbols, incoherent data, dashed curve, coherent theory; solid curve, incoherent theory.

The incoherent data are normalized to the same integrated FDCS as the coherent data so that no meaningful comparison in magnitude between the two data sets is possible. At the two smaller θ_p both the coherent and the incoherent data only exhibit a single peak

structure. This is the expected behavior because the direction of **q** is too close to $\theta_{el} = 0$ for the binary peak to be resolvable from the forward peak, regardless of the coherence length. Here, no large differences in shape between the two data sets can be discerned, although the peak structure in the coherent case appears to be somewhat narrower. At θ_p = 0.3 mrad a separate forward/binary double peak structure becomes visible in the coherent data. In the incoherent data, on the other hand, the minimum separating the forward and binary peaks is much shallower, if present at all, and the forward peak (relative to the binary peak) is strongly suppressed compared to the coherent data. At θ_p = 0.5 mrad the differences between the coherent and incoherent data become even larger. While in the coherent FDCS the double peak structure becomes even more pronounced, in the incoherent data the forward peak is still barely separated from the binary peak and even more suppressed compared to θ_p = 0.3 mrad. This is the more remarkable considering that with increasing θ_p the direction of **q** departs increasingly from 0^o. Furthermore, the binary peak in the incoherent data is shifted in the forward direction relative to the coherent data. In summary, the data suggest that coherence effects become stronger with increasing θ_p.

The dashed and solid lines in Figure 2 show our coherent and incoherent calculations. Significant discrepancies between experiment and theory are found, for both the coherent and incoherent cases. In the overall magnitude the calculation overestimates the coherent data by as much as a factor of 4. With increasing θ_p there are increasing discrepancies in the centroids of the maxima. Finally, the theoretical widths of the peak structures are too large, especially in the coherent case. These discrepancies could be partly due to the high sensitivity of the FDCS on the coherence length [49] combined with the uncertainty in the experimental coherence length and due to the lack of a proper description

of the electron capture channel in theory. However, qualitatively, there are two important features in which theory agrees with experiment: first, at small θ_p the differences between the coherent and incoherent calculations are relatively small, but with increasing θ_p they become much more prominent. Second, at $\theta_p = 0.5$ mrad the double peak structure seen in the coherent calculation turns into a single peak in the incoherent case, located between the forward and binary peaks of the coherent FDCS, like in the experimental data. Thus, theory provides some support for the interpretation that the double peak structure at large θ_p for the coherent FDCS is due to interference between the first- and higher-order amplitudes. It should be noted that in the theoretical model the interference emerges from a coherent superposition of different impact parameters leading to the same θ_p. In general, this does not necessarily require the presence of higher-order contributions [40,43]. However, in the present case in a pure first-order calculation the forward peak is completely absent. Furthermore, an incoherent higher-order calculation (considering only a small interval of impact parameters) lead to only one peak. Interference between various impact parameters is therefore equivalent to interference between first- and higher-order amplitudes.

In analogy to classical optics the coherent cross sections can be expressed as a product between the incoherent cross sections and the interference term, i.e. the ratio R between the coherent and incoherent FDCS represent the interference term. These ratios are plotted as a function of θ_{el} in Figure 3 for $\theta_p = 0.3$ and 0.5 mrad in the left and right panels, respectively. For the smaller scattering angles the differences between the coherent and incoherent FDCS are relatively small and the ratios mostly show statistical scatter. At $\theta_p = 0.3$ mrad the ratios show maxima at $\theta_{el} = 0^o$ and 35^o, which is close to the direction of **q** indicated by the vertical arrow. The peaks are separated by a shallow minimum at about

20°. At θ_p = 0.5 mrad the double peak structure is significantly more pronounced, where the ratio in the minimum is about a factor of 5 smaller than in the forward maximum. Due to the large error bars for large θ_{el} the location of the second maximum cannot be accurately determined, however, it seems to be consistent with the direction of **q** at 48°. These features in the interference term extracted from the experimental data further support the interpretation that the double peak structure observed in the coherent FDCS is due to constructive interference in the forward direction and in the direction of **q** and destructive interference in between these directions.

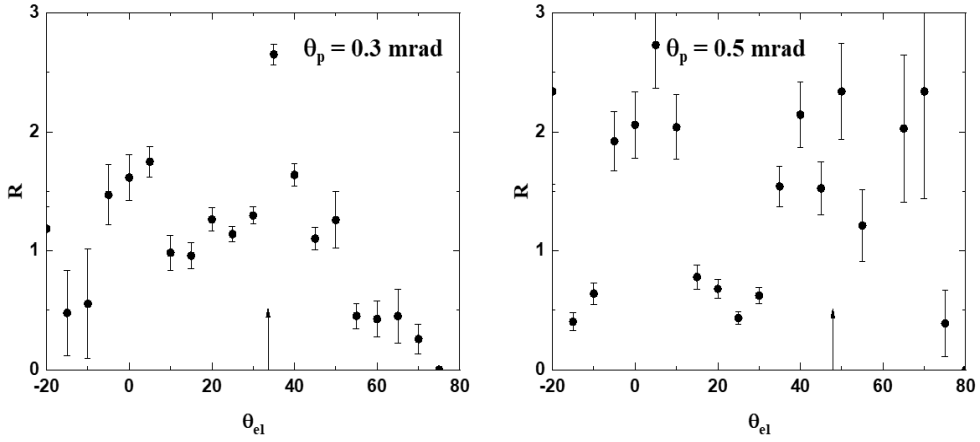

Figure 3. Ratios between the coherent and incoherent FDCS from Figure 1

Unfortunately, the theoretical ratios are dominated by the behavior in the wings of the maxima in the FDCS. As a result, the ratios are very large in regions (θ_{el} approaching -90° and 180°) where the FDCS are nearly 0, which covers the shape of the interference term in the interesting region of the double peak structure. Therefore, a comparison between theoretical and experimental ratios does not provide any further insight.

5. CONCLUSIONS AND OUTLOOK

We have measured and calculated FDCS for ionization in the velocity matching regime for an incoherent projectile beam and compared them to data previously taken for a coherent beam. With increasing scattering angle increasing differences between the coherent and incoherent FDCS are found. At the largest scattering angle these differences are of qualitative nature. A double peak structure in the coherent case is nearly turned into a single peak in the incoherent case, which is the behavior expected from a classical point of view. We therefore conclude that the double peak structure in the coherent FDCS is due to constructive interference in the forward direction and in the direction of **q** and destructive interference leading to a minimum between these directions. This conclusion is qualitatively supported by our calculations, although there are large quantitative discrepancies to the experimental data.

As an outlook, we plan to extend the experiments to other projectile energies and targets in order to investigate the interference leading to the double peak structure more systematically. On the theoretical side it appears important to include bound projectile states in the basis set to account for the capture channel. Due to unitarity the missing projectile states means that capture is erroneously counted as ionization in the transition amplitude. This effect is expected to have a particularly large impact in the velocity matching regime because of the energetic proximity of the continuum electron states to the bound projectile states. Unfortunately, including bound projectile states requires a major redesign of the existing model implying additional computational efforts and successfully concluding such a project is very time-consuming.

ACKNOWLEDGEMENTS

This work was supported by the National Science Foundation under grant no. PHY-2011307 and by the National Research Development and Innovation Office (NKFIH) grant no. KH 126886. The numerical calculations were performed using the high-performance computing resources of Babes-Bolyai University. S.B. was supported by the Babeș-Bolyai University under grant no. GTC 35280/18.11.2020.

REFERENCES

[1] T.N. Rescigno, M. Baertschy, W.A. Isaacs, and C.W. McCurdy, Science 286, 2474 (1999)

[2] M. Schulz, R. Moshammer, D. Fischer, H. Kollmus, D.H. Madison, S. Jones, and J. Ullrich, Nature 422, 48 (2003)

[3] M. Brauner, J.S. Briggs, and H. Klar, J. Phys. B 22, 2265 (1989)

[4] M.F. Ciappina, W.R. Cravero, and C.R. Garibotti, Phys. Rev. A 70, 062713 (2004)

[5] M. Foster, J.L. Peacher, M. Schulz, D.H. Madison, Z. Chen, and H.R.J. Walters, Phys. Rev. Lett. 97, 093202 (2006)

[6] C. Dal Cappello, Z. Rezkallah, S. Houamer, I. Charpentier, P.A. Hervieux, M.F. Ruiz Lopez, R. Dey, and A.C. Roy, Phys. Rev. A 84, 032711 (2011)

[7] K.A. Kouzakov, S.A. Zaytsev, Yu.V. Popov, and M. Takahashi, Phys. Rev.A 86, 03 2710 (2012)

[8] L. Czipa and L. Nagy, Phys. Rev. A 95, 062709 (2017)

[9] A.B. Voitkiv, Phys. Rev. A 95, 032708 (2017)

[10] L. Gulyás, S. Egri, and A. Igarashi, Phys. Rev. A 99, 032704 (2019)

[11] M.F. Ciappina, M.S. Pindzola, and J. Colgan, Phys. Rev. A 87, 042706 (2013)

[12] H.R.J. Walters and C.T. Whelan, Phys. Rev. A 89, 032709 (2014)

[13] S. Borbély, J. Feist, K. Tőkési, S. Nagele, L. Nagy, and J. Burgdörfer, Phys. Rev.A90, 052706 (2014)

[14] M. Baxter, T. Kirchner, and E. Engel, Phys. Rev. A 96, 032708 (2017)

[15] I.B. Abdurakhmanov, J.J. Bailey, A.S. Kadyrov, and I. Bray, Phys. Rev. A 97,032707 (2018)

[16] G.B. Crooks and M.E. Rudd, Phys. Rev. Lett. 25, 1599 (1970)

[17] L. Sarkadi, J. Palinkas, A. Köver, D. Berenyi, and T. Vajnai, Phys. Rev. Lett. 62, 527 (1989)

[18] T. Vajnai, A.D. Gaus, J.A. Brand, W. Htwe, D.H. Madison, R.E.Olson, J.L.Peacher, and M. Schulz, Phys. Rev. Lett. 74, 3588 (1995)

[19] L.C. Tribedi, P. Richard, W. Dehaven, L. Gulyás, M.W. Gealy, M.E. Rudd,Phys.Rev. A 58, 3619 (1998)

[20] Th. Weber, Kh. Khayyat, R. Dörner, V.D. Rodríguez, V. Mergel, O. Jagutzki, L. Schmidt, K.A. Müller, F. Afaneh, A. Gonzalez, and H. Schmidt-Böcking,Phys. Rev.Lett. 86, 224 (2001)

[21] L. Sarkadi, L. Gulyas, and L. Lugosi, Phys. Rev. A 65, 052715 (2002)

[22] M. Schulz, A.C. Laforge, K.N. Egodapitiya, J.S. Alexander, A. Hasan, M.F. Ciappina, A.C. Roy, R. Dey, A. Samolov, and A.L. Godunov, Phys. Rev. A 81, 052705 (2010)

[23] U. Chowdhury, M. Schulz, and D. H. Madison, Phys. Rev. A 83, 032712 (2011)

[24] H.R.J. Walters and C.T. Whelan, Phys Rev. A 92, 062712 (2015)

[25] A. Silvus, M. Dhital, S. Bastola, J. Buxton, Z. Klok, E. Ali, M.F. Ciappina, B. Boggs, D. Cikota, D.H. Madison, and M. Schulz, J. Phys. B 52, 125202 (2019)

[26] J. Ullrich, R. Moshammer, A. Dorn, R. Dörner, L. Schmidt, and H. Schmidt-Böcking, Rep. Prog. Phys. 66, 1463 (2003)

[27] R. Dörner, V. Mergel, O. Jagutzski, L. Spielberger, J. Ullrich, R. Moshammer, and H. Schmidt-Böcking, Phys. Rep. 330, 95 (2000)

[28] M. Schulz and D.H. Madison, Intern. J. Mod. Phys. A 21, 3649 (2006)

[29] H. Gassert, O. Chuluunbaatar, M. Waitz, F. Trinter, H.-K. Kim, T. Bauer, A. Laucke, Ch. Müller, J. Voigtsberger, M. Weller, J. Rist, M. Pitzer, S. Zeller, T. Jahnke, L. Ph. H.Schmidt, J. B. Williams, S. A. Zaytsev, A. A. Bulychev, K. A. Kouzakov, H. Schmidt Böcking, R. Dörner, Yu. V. Popov, and M. S. Schöffler, Phys. Rev. Lett. 116, 073201 (2016)

[30] N.V. Maydanyuk, A. Hasan, M. Foster, B. Tooke, E. Nanni, D.H. Madison, and M. Schulz, Phys. Rev. Lett. 94, 243201 (2005)

[31] M. Schulz, A. Hasan, N.V. Maydanyuk, M. Foster, B. Tooke, and D.H. Madison, Phys. Rev. A 73, 062704 (2006)

[32] A. Hasan, S. Sharma, T.P. Arthanayaka, B.R. Lamichhane, J. Remolina, S. Akula, D.H. Madison, and M. Schulz, J. Phys. B 47, 215201 (2014)

[33] M. Schulz, R. Moshammer, A.N. Perumal, and J. Ullrich, J. Phys. B 35, L161 (2002)

[34] M. Schulz, B. Najjari, A.B. Voitkiv, K. Schneider, X. Wang, A.C. Laforge, R. Hubele, J. Goullon, N. Ferreira, A. Kelkar, M. Grieser, R. Moshammer, J. Ullrich, and D. Fischer, Phys. Rev. A 88, 022704 (2013)

[35] M. Dhital, S. Bastola, A. Silvus, A. Hasan, B.R. Lamichhane, E. Ali, M.F. Ciappina, R.A. Lomsadze, D. Cikota, B. Boggs, D.H. Madison, and M. Schulz, Phys. Rev. A 99, 062710 (2019)

[36] M. Dhital, S. Bastola, A. Silvus, B.R. Lamichhane, E. Ali, M.F. Ciappina, R. Lomsadze, A. Hasan, D.H. Madison, and M. Schulz, Phys. Rev. A 100, 032707 (2019)

[37] K.N. Egodapitiya, S. Sharma, A. Hasan,A.C. Laforge, D.H. Madison, R. Moshammer, and M. Schulz, Phys. Rev. Lett. 106, 153202(2011)

[38] M. Schulz in "Advances in Atomic, Molecular, and Optical Physics" 66, 508-543, edited by E. Arimondo, C.C. Lin, and S. Yelin, Elsevier, Amsterdam (2017)

[39] R.O. Barrachina, F. Navarrete, M.F. Ciappina, Phys. Res. 2, 043353 (2020)

[40] L. Nagy, F. Jarai-Szabo, S. Borbely, J. Phys. B 51, 144005 (2018)

[41] L. Sarkadi, I. Fabre, F. Navarrete, and R.O. Barrachina, Phys. Rev. A 93, 032702 (2016)

[42] A.D. Gaus, W. Htwe, J.A. Brand, T.J. Gay, and M. Schulz, Rev. Sci. Instrum. 65, 3739 (1994)

[43] L. Nagy, F. Jarai-Szabo, S. Borbely, T. Arthanayaka, B.R. Lamichhane, A. Hasan, and M. Schulz, in "The State-of-The-Art-Reviews on Energetic Ion-Atom and Ion Molecule Collisions", Volume 2, edited by Dz. Belkic, I. Bray and A. Kadyrov, p. 129, World Scientific Publishing (2019)

[44] J. Feist, S. Nagele, R. Pazourek, E. Persson, B. I. Schneider, L. A. Collins, and J. Burgdörfer, Phys. Rev. A 77, 043420 (2008)

[45] T. N. Rescigno and C. W. McCurdy, Phys. Rev. A 62, 032706 (2000)

[46] T. J. Park and J. C. Light, J. Chem. Phys. 85, 5870 (1986)

[47] S. Borbély, X.-M. Tong, S. Nagele, J. Feist, I. Březinová, F. Lackner, L. Nagy, K. Tőkési, J. Burgdörfer, Phys. Rev. A 98, 012707 (2018)

[48] R. Rivarola and P. Fainstein, Nucl. Instrum. Meth. Phys. Res. B. 205, 448 (2003).

[49] T. Arthanayaka, B.R. Lamichhane, A. Hasan, S. Gurung, J. Remolina, S. Borbély, F. Járai Szabó, L. Nagy, and M. Schulz, J. Phys. B 49, 13LT02 (2016)

SECTION

2. CONCLUSIONS AND OUTLOOK

2.1. CONCLUSIONS

From the date of its discovery interference and coherence effects (initially in optics and more recently in particle collisions) have unfolded many mysteries in Physics and other branches of science. It is now well established that features observed e.g., in cross-sections for the fragmentation processes can be very sensitive to such effects. Especially for fast and heavy ions, which have a small de Broglie wavelength, many studies [31, 39-42] show that FDCS could be affected by the projectile coherence properties. Theoretical studies [48, 60-62] also support these findings. The motivation for the experiments described in this dissertation was not to provide additional evidence for the existence of the projectile coherence effects, but rather we used it as a sensitive tool to study the dissociative capture process and explain the π - phase shift we obtained in a previous experiment [34].

Kinematically complete experiments were performed for 75keV p + H_2 collision in the Accelerator lab at the Missouri S&T Physics Department. Fully differential cross-sections were extracted for two different molecular orientations, namely the perpendicular and parallel orientations. Compared to a previous nearly kinematically complete experiment [34] we improved the recoil momentum resolution by a factor of 5 and enhanced the number of true coincidences by an order of magnitude. We also did a correction for the momentum transferred to the molecule which was neglected in the past. The detail can be found in data analysis section of the Paper-I. The FDCS showed

significant differences in the parallel and perpendicular orientations; especially in the case of parallel orientation a clear interference structure was observed. As compared to the previous results of Lamichane et al. [34] in the case of the parallel orientation, the interference structure is significantly more pronounced as can be seen in Figure 2 in the publication section (Paper I).

Although we found a pronounced two-center interference structure in both experimental data and theoretical calculations, there are significant differences. In the previous experiment, we investigated the same process and the same kinematics, but the cross-sections were integrated over the entire KER region (0-2 eV) for vibrational dissociation [34]. There, a constant phase shift of π for all values of θ_p was observed. Our present results show that the phase shift actually varies between 0 and π. It is π for relatively small θ_p and almost 0 for large θ_p. On the other hand, we found that the phase shift is nearly independent of KER in contrast to the theoretical calculations which indicated that the position of interference extrema significantly depends on the KER. We offered a hypothetical explanation for the θ_p dependent phase shift based on a classical analogy. Classically, a wave reflected from a fixed end will undergo a π phase shift. The quantum mechanical analogy is a reflection of a wave packet from an infinite potential wall, a scenario that is approximately realized by the molecular potential at small internuclear distances. After the excitation of the nuclear motion, the resulting vibrational wave packet can propagate either toward large internuclear distances which directly leads to the dissociation of the molecule (direct path), or towards small internuclear distances. When the wave packet travels to a small internuclear distance then the only way the molecule can dissociate is by reflecting from the potential wall (reflection path) which leads to the phase

shift in the interference term. The variation of the phase shift with θ_p can be explained using the classical concept of the inverse relation between impact parameter and scattering angle which is given in detail in the results and discussion part of the publication section (Paper I). In short, the argument is that relatively small (but not too small) θ_p should favor the reflection path, and large θ_p favor the direct path as illustrated in Figure 3 and Figure 4 (Paper I). In our hypothetical model, both paths should occur with similar probabilities in the case of very small θ_p, which explains the reduced interference pattern in the region.

In the second major project, we measured and calculated FDCS for the ionization of He using a 75keV proton beam with a small coherence length close to the dimension of the Helium atom. The experimental setup is similar to Dhital et al. except that the coherence length was significantly smaller than in the previous experiment [52]. We analyzed ejected electrons whose speed closely matches the speed of the incoming projectile (corresponding to a 68.5 eV energy loss), and this is called the velocity matching regime. The results reported in [52] showed a pronounced two-peak structure, one is the binary peak slightly displaced in the forward direction from the direction of **q**, and another occurs in the forward direction in the fully differential angular distribution. Classically, no double-peak structure is expected. As a hypothetical explanation, Dhital et. al. proposed interference between 1st and higher-order amplitudes. If this hypothesis is correct the double-peak structure should be less pronounced under less coherent experimental conditions, and this is indeed reflected in the FDCS in our current experimental data. At the largest scattering angle, a double peak structure in the coherent case is nearly turned into a single peak in the incoherent data. This supports the hypothesis of Dhital et. al. that a double peak in our previous data was caused by constructive interference between first and higher-order terms in the binary and

forward peak and the destructive interference leads to the minimum between them. This is further supported qualitatively by a theoretical model that accounts for the projectile coherence properties in terms of the width of the wave packet describing the projectile. However, there are significant quantitative discrepancies between theoretical and experimental FDCS.

2.2. OUTLOOK

Regarding the project on dissociative capture, if our explanation for the phase shift is confirmed it is different from the reason for a similar (but constant) phase shift observed in dissociation following electronic excitation to an antisymmetric dissociative state, where the explanation is based on parity conservation [5]. At this point, we do not claim conclusive evidence for the validity of our model. We hope our explanation would trigger further theoretical studies which will in the future either confirm or dismiss our model. From an experimental point of view, we already performed a kinematically complete experiment. So, a conceptually a more complete experiment offering additional information is not possible. However, we do plan to study this topic more systematically by varying projectile energy and repeating the experiments for other molecules.

Furthermore, we plan to expand our incoherent ionization experiment with He to a few other projectile energy losses both well below and above the velocity matching regime to study higher-order mechanisms other than PCI. Also, in the theoretical study included in Paper-II of the publication section, the bound projectile state was not included to account for the capture channel. As a result, capture was erroneously counted as ionization due to

unitarity which is expected to have a particularly large impact in the velocity matching regime. Therefore, non-perturbative approaches including bound projectile states in the basis set are called for.

BIBLIOGRAPHY

[1] T.N. Rescigno, M. Baertschy, W.A. Isaacs, and C.W. McCurdy, Science 286, 2474 (1999)

[2] T. F. Tuan and E. Gerjuoy, Phys. Rev. 117, 756 (1960)

[3] S. Cheng, C. L. Cocke, V. Frohne, E. Y. Kamber, J. H. McGuire, and Y. Wang, Phys. Rev. A 47, 3923 (1993)

[4] N. Stolterfoht, B. Sulik, V. Hoffmann, B. Skogvall, J. Y. Chesnel, J. Ragnama, F. Frèmont, D. Hennecart, A. Cassimi, X. Husson, A. L. Landers, J. Tanis, M. E. Galassi, and R. D. Rivarola, Phys. Rev. Lett. 87, 23201 (2001).

[5] D. S. Milne-Brownlie, M. Foster, J. Gao, B. Lohmann, and D. H. Madison, Phys. Rev. Lett. 96, 233201 (2006)

[6] D. Misra, U. Kadhane, Y.P. Singh, L.C. Tribedi, P.D. Fainstein, and P. Richard Phys. Rev. Lett. 92, 153201 (2004)

[7] E.M. Staicu Casagrande, A. Naja, F. Mezdari, A. Lahmam-Bennani, P. Bolognesi, B. Joulakian, O. Chuluunbaatar, O. Al-Hagan, D. H. Madison, D.V. Fursa and I. Bray, J. Phys. B 41, 025204 (2008)

[8] H. T. Schmidt, D. Fischer, Z. Berenyi, C.L. Cocke, M. Gudmundsson, N. Haag, H.A.B. Johansson, A. Källberg, S.B. Levin, P. Reinhed, U. Sassenberg, R. Schuch, A. Simonsson, K. Stöchkel, and H. Cederquist, Phys. Rev. Lett. 101, 083201 (2008)

[9] H. Ehrhardt, K. Jung, G. Knoth, and P. Schlemmer, Z. Phys. D, Z. Phys. D 1, 3 (1986).

[10] I. Bray, J. Phys. B 33, 581 (2000).

[11] J. Colgan, M. S. Pindzola, Phys. Rev. A 74, 012713 (2006).

[12] C. Froese-Fischer, T. Brage, and P. Johnsson, Computational Atomic Structure: AnMCHF Approach, CRC Press (1997)

[13] A. Messiah, Quantum Mechanics (North-Holland, Amster- dam, 1970), Vol. II.

[14] S. F. Zhang, D. Fischer, M. Schulz, A. B. Voitkiv, A. Senftleben, A. Dorn, J. Ullrich, X. Ma, and R. Moshammer, Phys. Rev. Lett. 112, 023201 (2014).

[15] M. F. Ciappina, W. R. Cravero, M. Schulz, R. Moshammer, and J. Ullrich, Phys.Rev. A 74, 042702 (2006).

[16] A. B. Voitkiv and B. Najjari, Phys. Rev. A 79, 022709 (2009).

[17] D. H. Madison, D. Fischer, M. Foster, M. Schulz, R. Moshammer, S. Jones, and J. Ullrich, Phys. Rev. Lett. 91, 253201 (2003).

[18] H. Ehrhardt, M. Schulz, T. Tekaat, and K. Willmann, Phys. Rev. Lett. 22, 89 (1969).

[19] M. Schulz, M. F. Ciappina, T. Kirchner, D. Fischer, R. Moshammer, and J. Ullrich, Phys. Rev. A 79, 042708 (2009).

[20] M. Schulz, Phys. Scr. 80, 068101 (2009).

[21] M. Schulz, R. Moshammer, D. Fischer, H. Kollmus, D. H. Madison, S. Jones, and J. Ullrich, Nature(London) 422, 48 (2003).

[22] M. Schulz and D. H. Madison, Int. J. Mod. Phys. A 21, 3649 (2006).

[23] T.N. Rescigno, M. Baertschy, W.A. Isaacs, and C.W. McCurdy, Science 286, 2474 (1999).

[24] M. Dürr, C. Dimopoulou, A. Dorn, B. Najjari, I. Bray, D. V. Fursa, Z. Chen, D. H. Madison, K. Barschat, and J. Ullrich, Journal of Physics B. 39, 4097 (2006)

[25] M. Dürr, C. Dimopoulou, A. Dorn, B. Najjari, K. Barschat, I. Bray, D. V. Fursa, Z. Chen, D. H. Madison, and J. Ullrich, Phys. Rev. A 77, 032717 (2008)

[26] X. Ren, A. Senftleben, T. Pflüger, A. Dorn, J. Colgan, M.S. Pindzola, O. Al Hagan, D. H. Madison, I. Bray, D. V. Fursa, and J. Ullrich, Phys. Rev. A, 82, 032712 (2010)

[27] R. Dörner, V. Mergel, R. Ali, U. Buck, C.L. Cocke, K. Froschauer, O. Jagutzki, S. Lencinas, W.E. Meyerhof, S. Nüttgens, R. E. Olson, H. Schmidt-Böcking, L. Spielberger, K. Tökesi, J. Ullrich, M. Unverzagt, and W. Wu, Phys. Rev. Lett. 72, 3166 (1994).

[28] A. Igarashi and L. Gulyas, J. Phys. B 50, 035201 (2017)

[29] L. Sarkadi, I. Fabre, F. Navarrete, and R. Barrachina, Phys. Rev. A 93, 032702 (2016)

[30] L. Ph. H. Schmidt, S. Schössler, F. Afaneh, M. Schöffler, K. E. Stiebing, H. Schmidt-Böcking, and R. Dörner, Phys. Rev. Lett. 101, 173202 (2008).

[31] K. N. Egodapitiya, S. Sharma, A. Hasan, A. C. Laforge, D. H. Madison, R. Moshammer, and M. Schulz, Phys. Rev. Lett. 106, 153202 (2011).

[32] F. Navarrete, M.F. Ciappina, L. Sarkadi, and R.O. Barrachina, Nucl. Instrum. Meth. B, 408, 165 (2017)

[33] M. Schulz in "Advances in Atomic, Molecular, and Optical Physics", Vol. 66, p. 508 edited by E. Arimondo, C.C. Lin, and S. Yelin, Elsevier, Cambridge MA, USA (2017)

[34] B.R. Lamichhane, T. Arthanayaka, J. Remolina, A. Hasan, M.F. Ciappina, F. Navarrete, R.O. Barrachina, R.A. Lomsadze, and M. Schulz, Phys. Rev. Lett. 119, 083402 (2017)

[35] S. Bastola, M. Dhital, B. Lamichhane, A. Silvus, R. Lomsadze, J. Davis, A. Hasan, A. Igarashi, and M. Schulz Phys. Rev. A 105, 032805 (2022)

[36] B. Lamichane's doctoral thesis "Fully differential study of dissociative capture in p + H2 collisions" (Missouri S&T, 2018)

[37] M.F. Ciappina and R.D. Rivarola, J. Phys. B 41, 015203 (2008)

[38] U. Chowdhury, M. Schulz, and D. H. Madison, Phys. Rev. A 83, 032712 (2011)

[39] S. Sharma, T.P. Arthanayaka, A. Hasan, B.R. Lamichhane, J. Remolina, A. Smith, and M. Schulz, Phys. Rev., A 89, 052703 (2014)

[40] S. Sharma, T.P. Arthanayaka, A. Hasan, B.R. Lamichhane, J. Remolina, A. Smith, and M. Schulz, Phys. Rev. A 90, 052710 (2014)

[41] T. P. Arthanayaka's doctoral thesis "Fully differential study of projectile coherence effects in the ionization of molecular hydrogen and atomic helium"

[42] T.P. Arthanayaka, S. Sharma, B.R. Lamichhane, A. Hasan, J. Remolina, S. Gurung, and M. Schulz, J. Phys. B 48, 071001 (2015)

[43] T. Arthanayaka, B.R. Lamichhane, A. Hasan, S. Gurung, J. Remolina, S. Borbély, F. Járai Szabó, L. Nagy, and M. Schulz, J. Phys. B 49, 13LT02 (2016)

[44] Borbély S, Feist J, Tőkési K, Nagele S, Nagy L and Burgdörfer J 2014 Phys. Rev. A 90052706

[45] B. R. Lamichhane, A. Hasan, T. Arthanayaka, M. Dhital, K. Koirala, T. Voss, R. A. Lomsadze, and M. Schulz, Phys. Rev. A 96, 042708 (2017).

[46] A. Senftleben, T. Pflüger, X. Ren, O. Al-Hagan, B. Najjari, D. Madison, A. Dorn, and J. Ullrich, J. Phys. B 43, 081002 (2010).

[47] T. E. Sharp, At. Data Nucl. Data Tables 2, 119 (1970).

[48] A. Igarashi and L. Gulyas, J. Phys. B 52, 075204 (2019)

[49] A. Igarashi, J. Phys. B 53, 225205 (2020).

[50] G. B. Crooks and M. E. Rudd, Phys. Rev. Lett. 25, 1599 (1970)

[51] L. Sarkadi, J. Palinkas, A. Kover, D. Berenyi, and T. Vajnai, Phys. Rev. Lett. 62, 527 (1989)

[52] M. Dhital, S. Bastola, A. Silvus, B. R. Lamichhane, E. Ali, M. F. Ciappina, R. Lomsadze, A. Hasan, D. H. Madison, and M. Schulz, Phys. Rev. A 100, 032707 (2019).

[53] T. Vajnai, A. D. Gaus, J. A. Brand, W. Htwe, D. H. Madison, R. E. Olson, J. L. Peacher, and M. Schulz, Phys. Rev. Lett. 74, 3588 (1995)

[54] M. Dhital's Doctoral Thesis "Fully differential study of higher-order contributions to the few-body dynamics of simple atomic systems" (Missouri S&T, Fall 2020)

[55] A. Hasan, T. Arthanayaka, B.R. Lamichhane, S. Sharma, S. Gurung, J. Remolina, S. Akula, D.H. Madison, M.F. Ciappina, R.D. Rivarola, and M. Schulz, J. Phys. B 49, 04LT01 (2016)

[56] M.F. Ciappina, C.A. Tachino, R.D. Rivarola, S. Sharma, and M, Schulz, J. Phys. B 48, 115204 (2015)

[57] M. Dhital, S. Bastola, A. Silvus, A. Hasan, B.R. Lamichhane, E. Ali, M.F. Ciappina, R.A. Lomsadze, D. Cikota, B. Boggs, D.H. Madison, and M. Schulz, Phys. Rev. A 99, 062710 (2019)

VITA

Sujan Bastola was born in Kathmandu, Nepal and raised at an early age in Lamjung, Nepal and later in Kathmandu, Nepal. He completed high school at Edmark Academy in Kathmandu, Nepal. He received his Bachelor of Science in Physics from Tribhuvan University in July 2008. He then received a Master of Science in Physics from Tribhuvan University in December 2012.

He started a new chapter of his life after joining Missouri S&T as a Ph.D. student in 2017. He spent his four and half years in Accelerator Lab experimenting with many projects to study the few-body dynamics using atomic collisions experiments under the guidance of Chancellor's Professor of Physics, Dr. Michael Schulz. He received his Doctor of Philosophy in Physics for his work on "USING COHERENCE AND INTERFERENCE TO STUDY THE FEW BODY DYNAMICS IN SIMPLE ATOMIC COLLISIONS SYSTEMS" from Missouri S&T in July 2022. He presented his research work at 32nd International Conference on Photonic, Electronic, and Atomic Collisions in July 2021 and at the 74th Annual Gaseous Electronics Conference in October 2021. He was awarded second prize at the 28th Annual Schearer Prize for his research presentation in Fall 2021 by Missouri S&T Physics Department.

He was involved in many voluntary activities around Rolla, MO during his graduate study at Missouri S&T. He volunteered as a science judge in a middle school science competition and participated as an exhibitor in diversity-related activities in another middle school near Rolla, MO.